ATHIC2023

Measurements of light hypernuclei properties and production yields in Au+Au collisions from the STAR experiment

Xiujun Li
(*for the STAR collaboration*)
University of Science and Technology of China
University of Tsukuba

Supported in part by the
U.S. DEPARTMENT OF ENERGY | Office of Science

Outline

- Introduction
- Hypernuclei measurements in STAR BES-II
  - Internal structure

    Branching ratios, lifetimes
  - Production mechanism

    Yields, particle ratios, directed flow
- Summary and outlook

Introduction: what and why

- What are hypernuclei?
  - Bound nuclear systems of non-strange and strange baryons

${}^{3}_{\Lambda}\mathrm{H}$

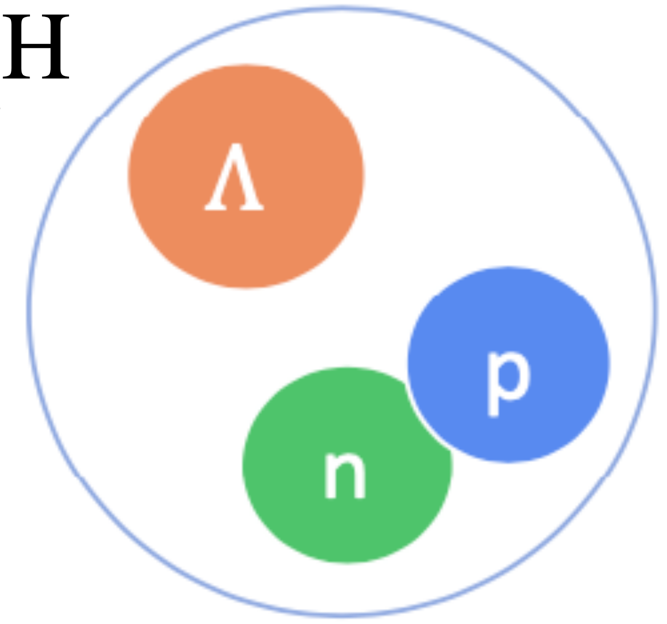

${}^{4}_{\Lambda}\mathrm{H}$

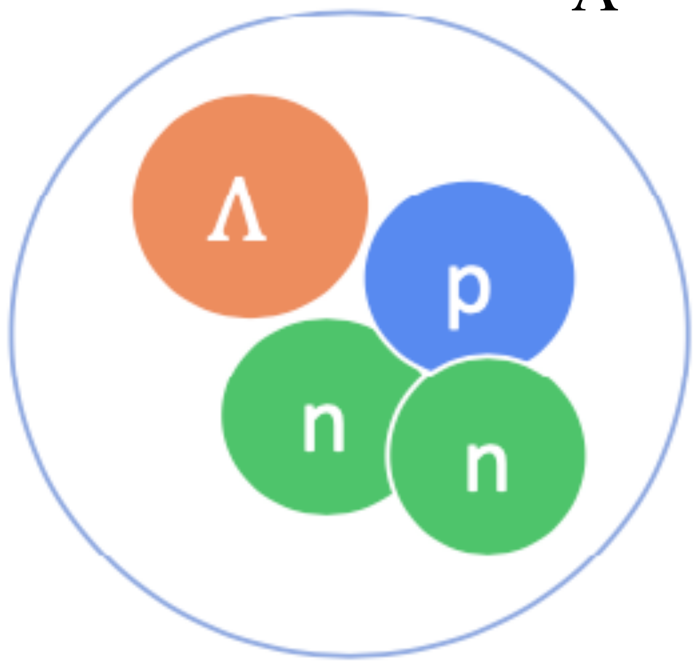

${}^{4}_{\Lambda}\mathrm{He}$

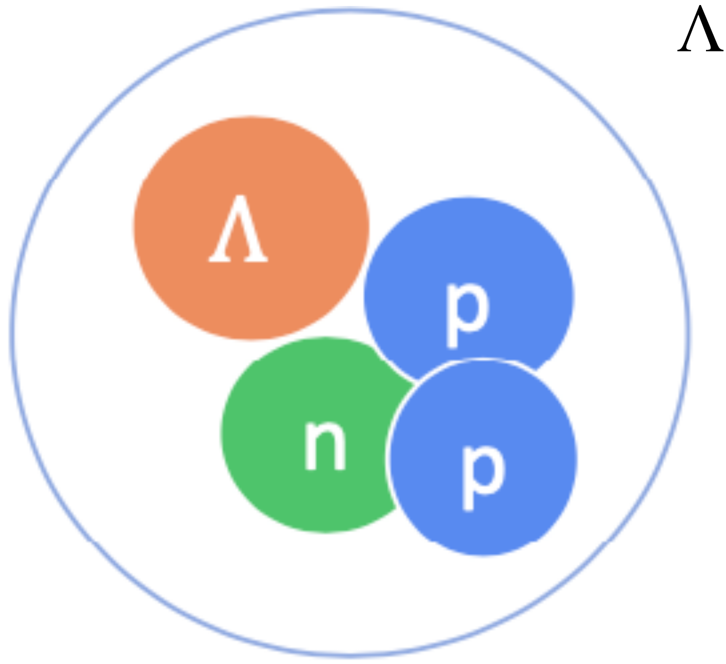

Marian Danysz (right) and Jerzy Pniewski (left) discovered hypernuclei in 1952

- Why hypernuclei?
  - Probe hyperon-nucleon (Y-N) interaction
  - Strangeness in high density nuclear matter
    - Equation-of-State (EoS) of neutron star

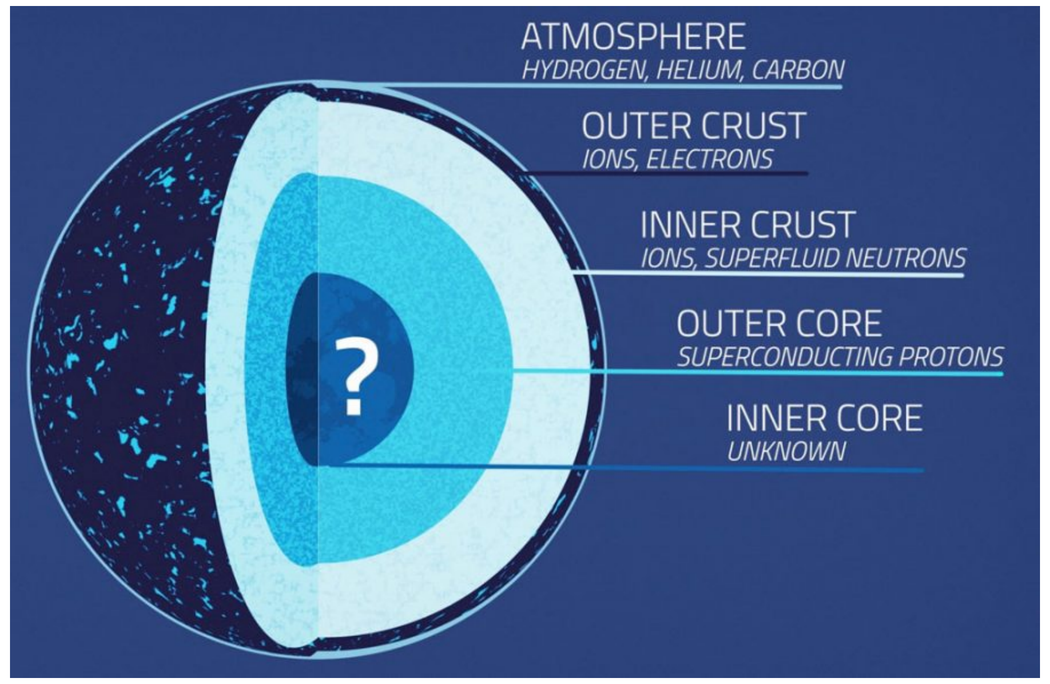

neutron star

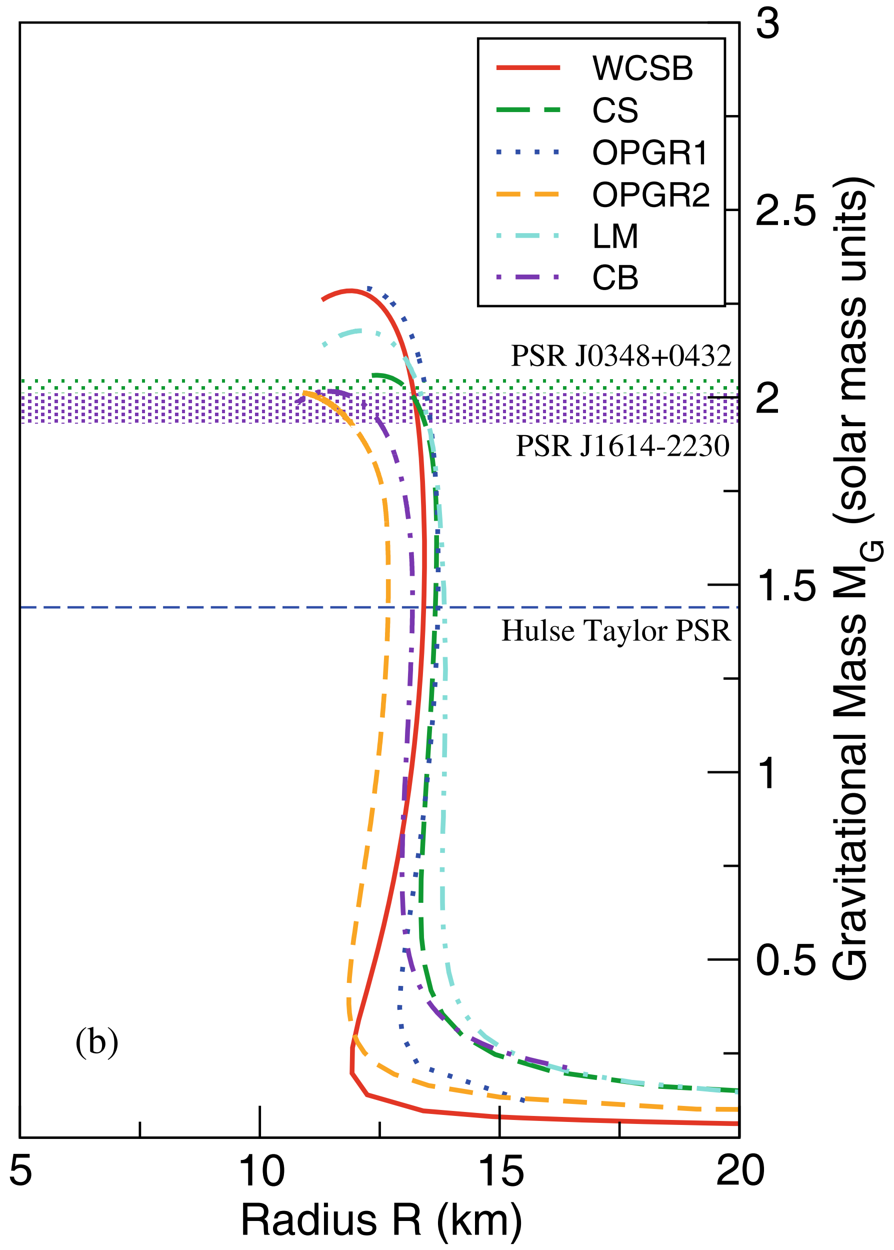

D. Chatterjee, Eur. Phys. J. A (2016) 52: 29

Introduction: how

- Experimentally, we can make measurements related to:

1. Internal structure

    - Lifetime, binding energy, branching ratios etc.

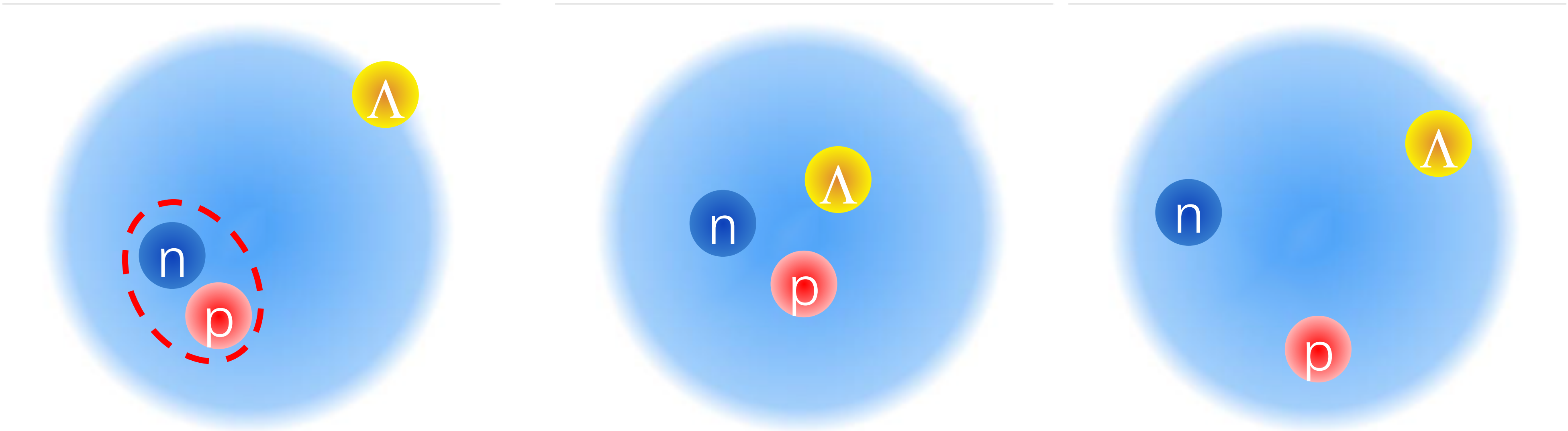

Understanding hypernuclei structure can provide insights to the Y-N interaction

2. Production mechanism

    - Spectra, collectivity etc.

The process of hypernuclei formation in violent heavy-ion collisions is not well understood

Introduction: RHIC BES program

- During the BES-II program, STAR utilized the fixed-target (FXT) setup, which extends the energy reach below $\sqrt{s_{NN}}$ = 7.7 GeV, down to 3.0 GeV

FXT mode setup of STAR detector :

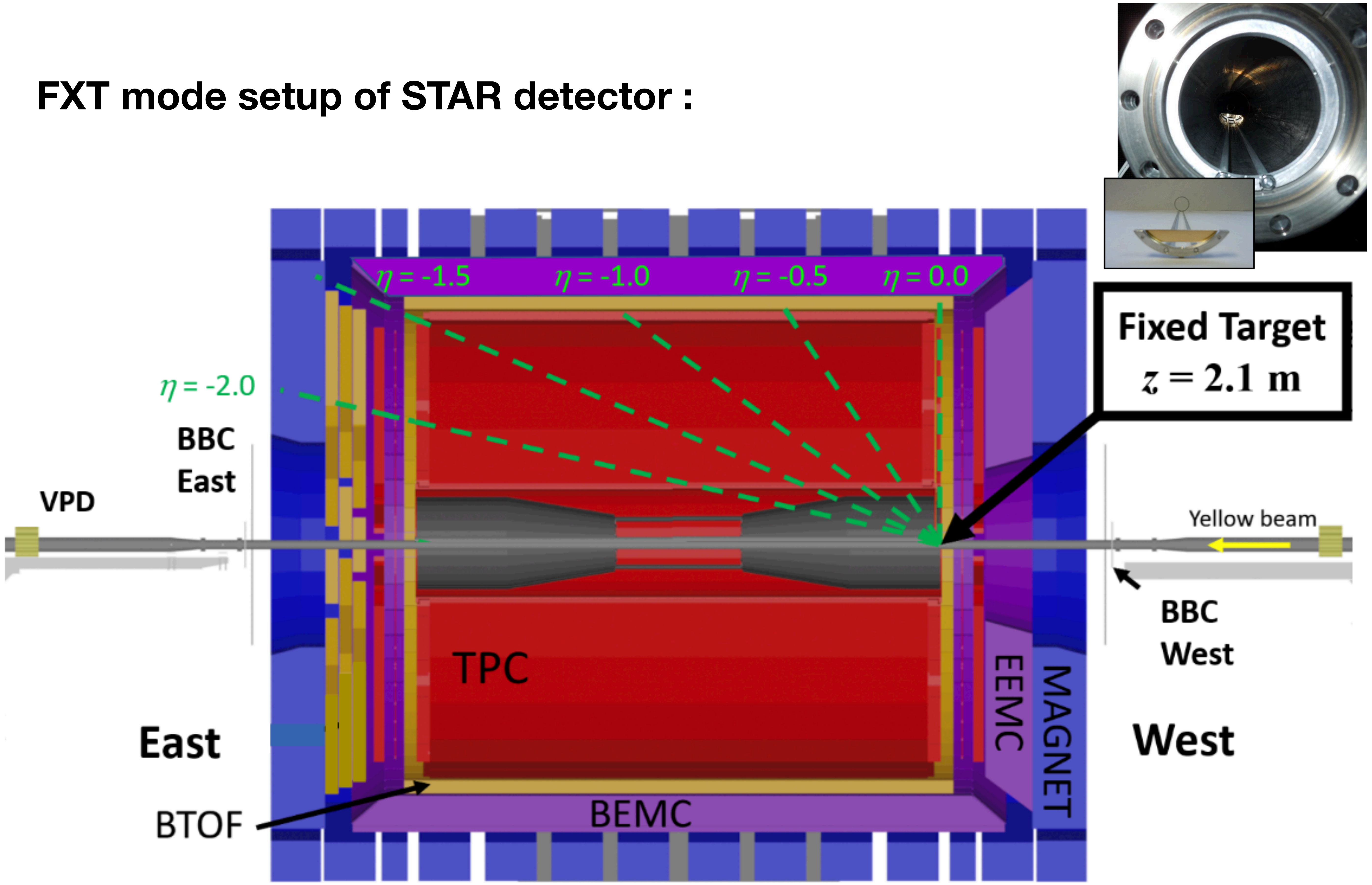

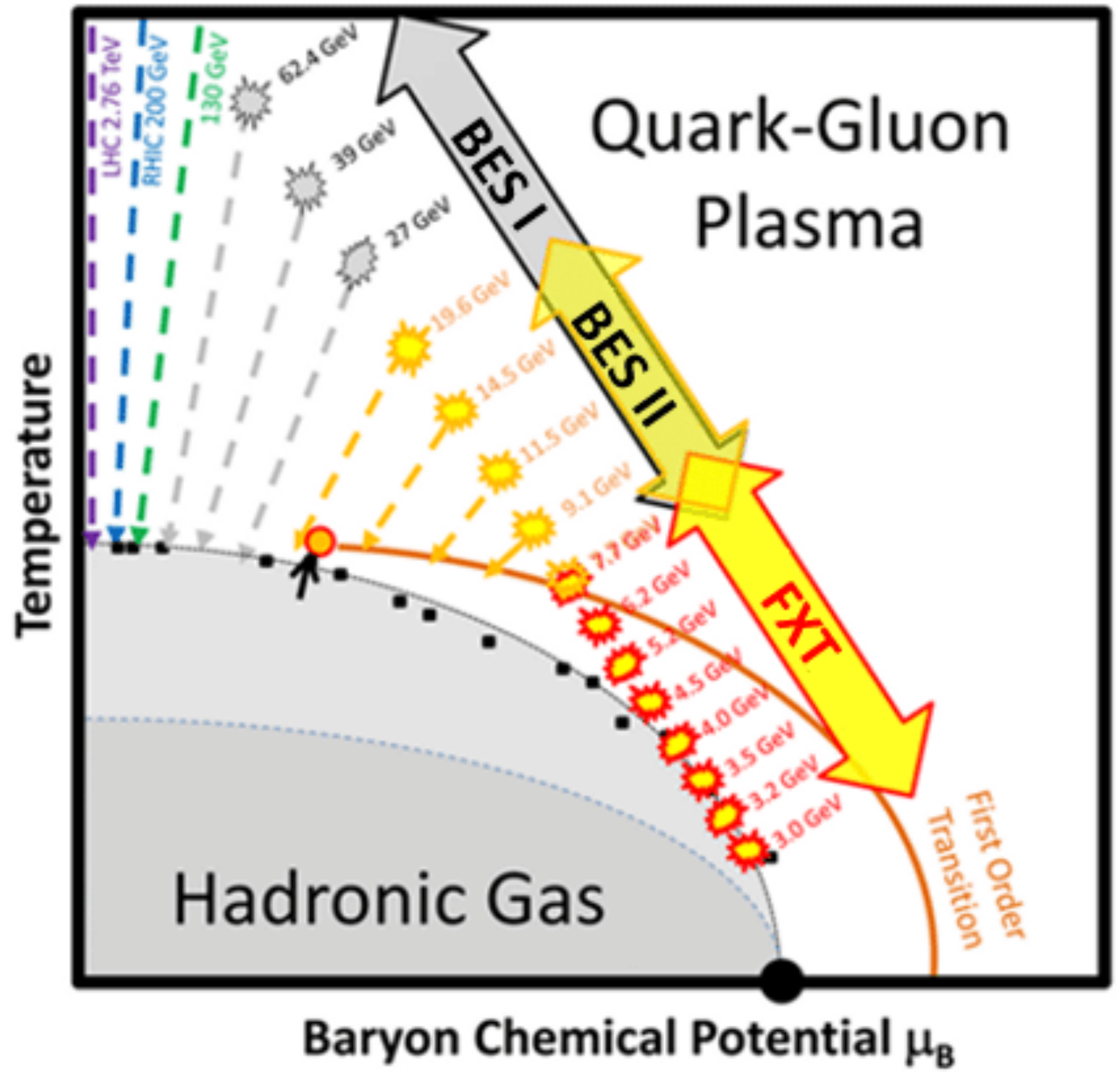

Introduction: hypernuclei and STAR BES-II

- **Hypernuclei measurements are scarce in heavy-ion collision experiments**

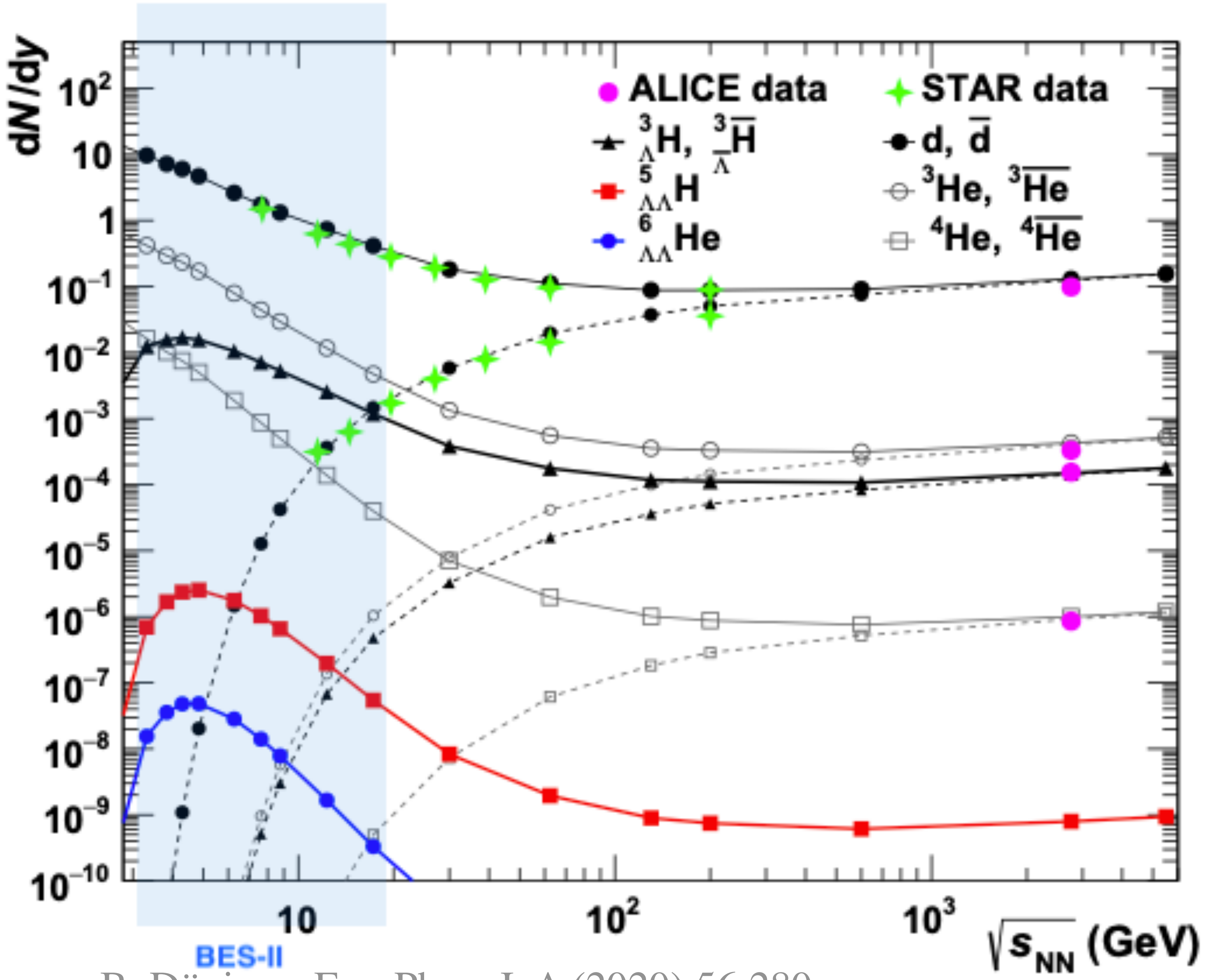

B. Dönigus, Eur. Phys. J. A (2020) 56:280
A. Andronic et al. PLB (2011) 697:203–207

- At low beam energies, hypernuclei production is expected to be enhanced due to high baryon density
- Datasets with large statistics taken during BES-II

→ A great opportunity to study hypernuclei production

List of BES-II datasets:

Year	$\sqrt{s_{NN}}$ [GeV]	Events
2018	27	555 M
	3.0	258 M
	7.2	155 M
2019	19.6	478 M
	14.6	324 M
	3.9	53 M
	3.2	201 M
	7.7	51 M
2020	11.5	235 M
	7.7	113 M
	4.5	108 M
	6.2	118 M
	5.2	103 M
	3.9	117 M
	3.5	116 M
	9.2	162 M
	7.2	317 M
2021	7.7	101 M
	3.0	2103 M
	9.2	54 M
	11.5	52 M
	13.7	51 M
	17.3	256 M
	7.2	89 M

Particle identification and hypernuclei reconstruction

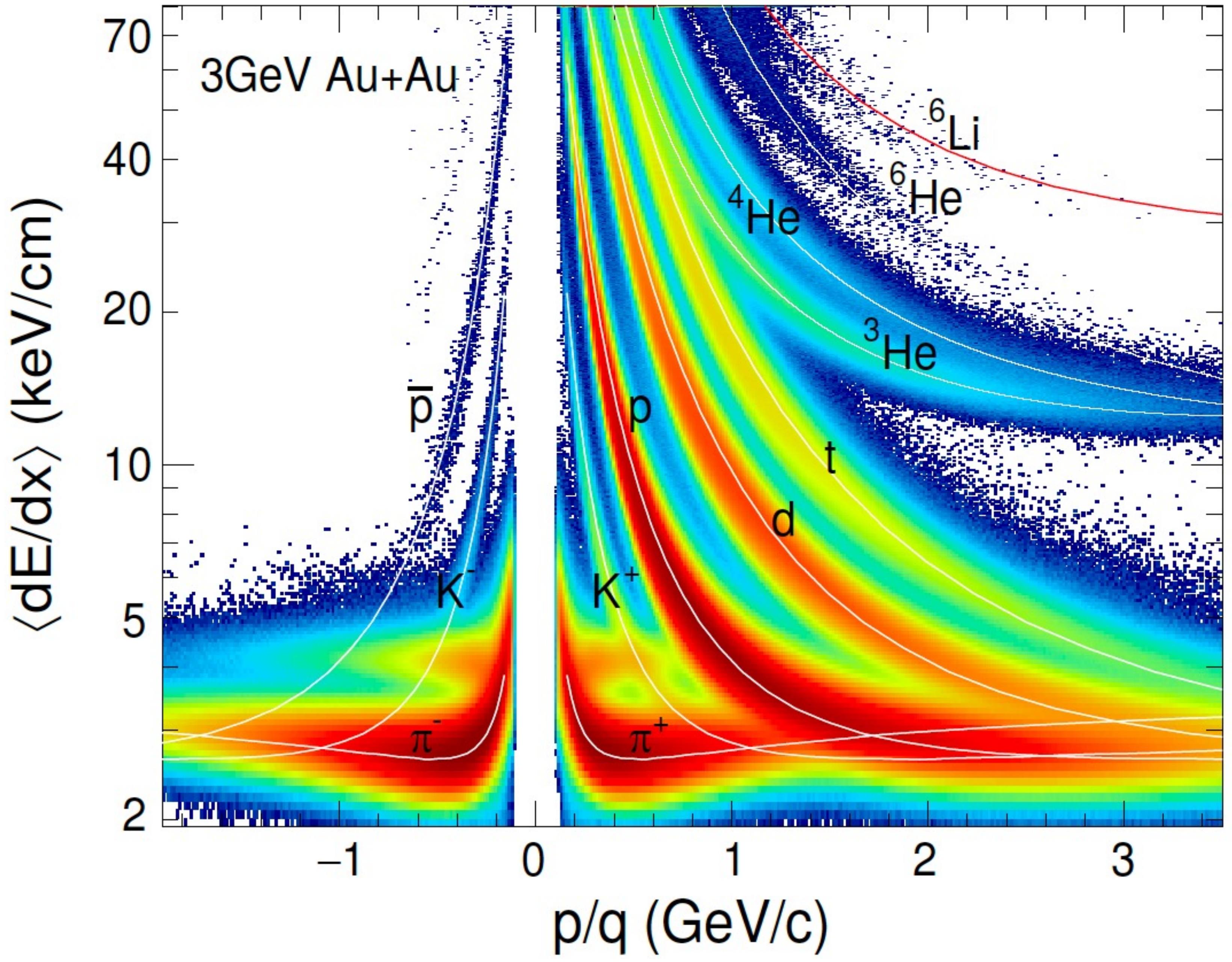

$^{3}_{\Lambda}\mathrm{H}\rightarrow \mathrm{d}+\mathrm{p}+\pi^{-}$:

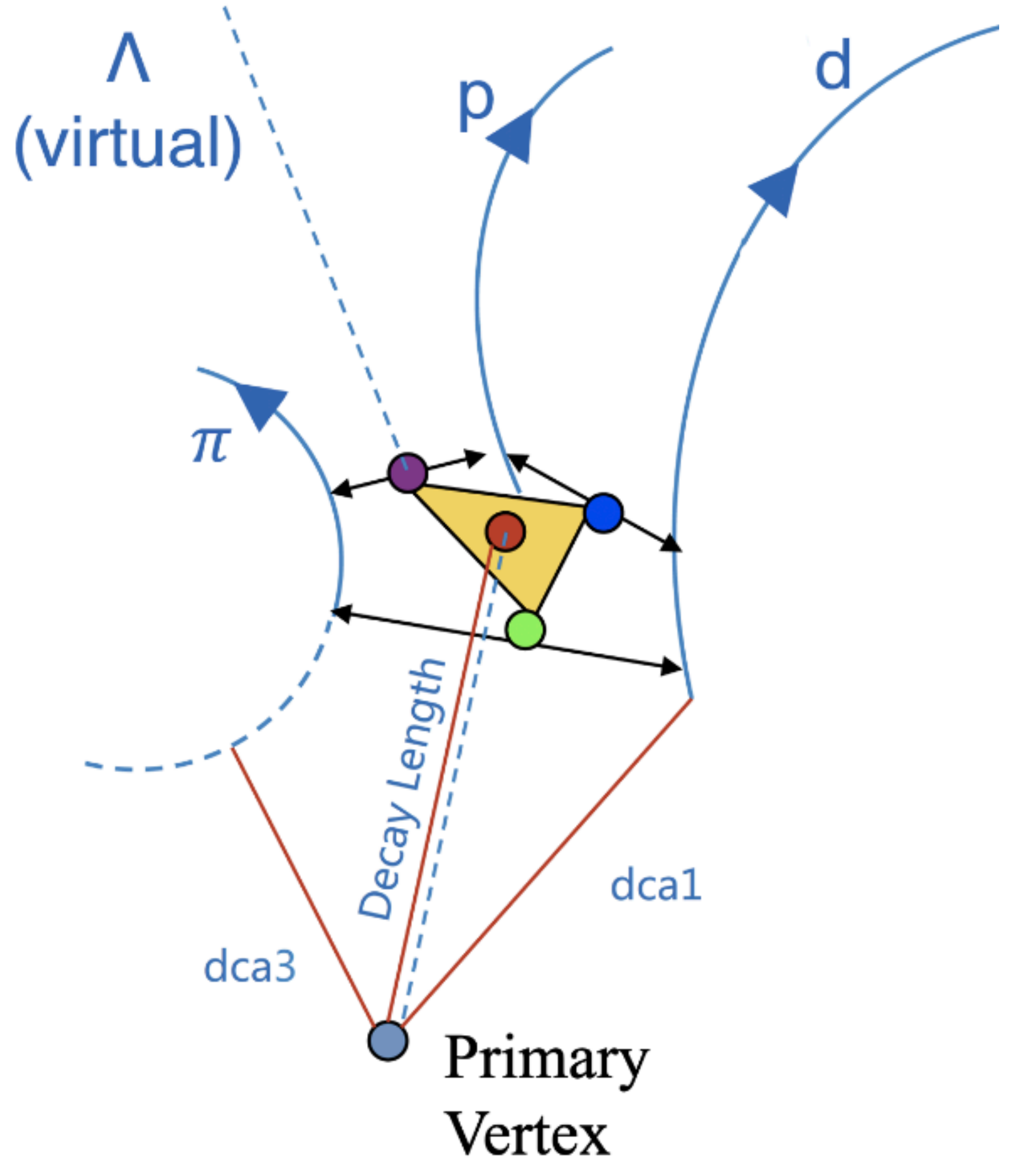

$^{3}_{\Lambda}\mathrm{H}\rightarrow {}^{3}\mathrm{He}+\pi^{-}$:

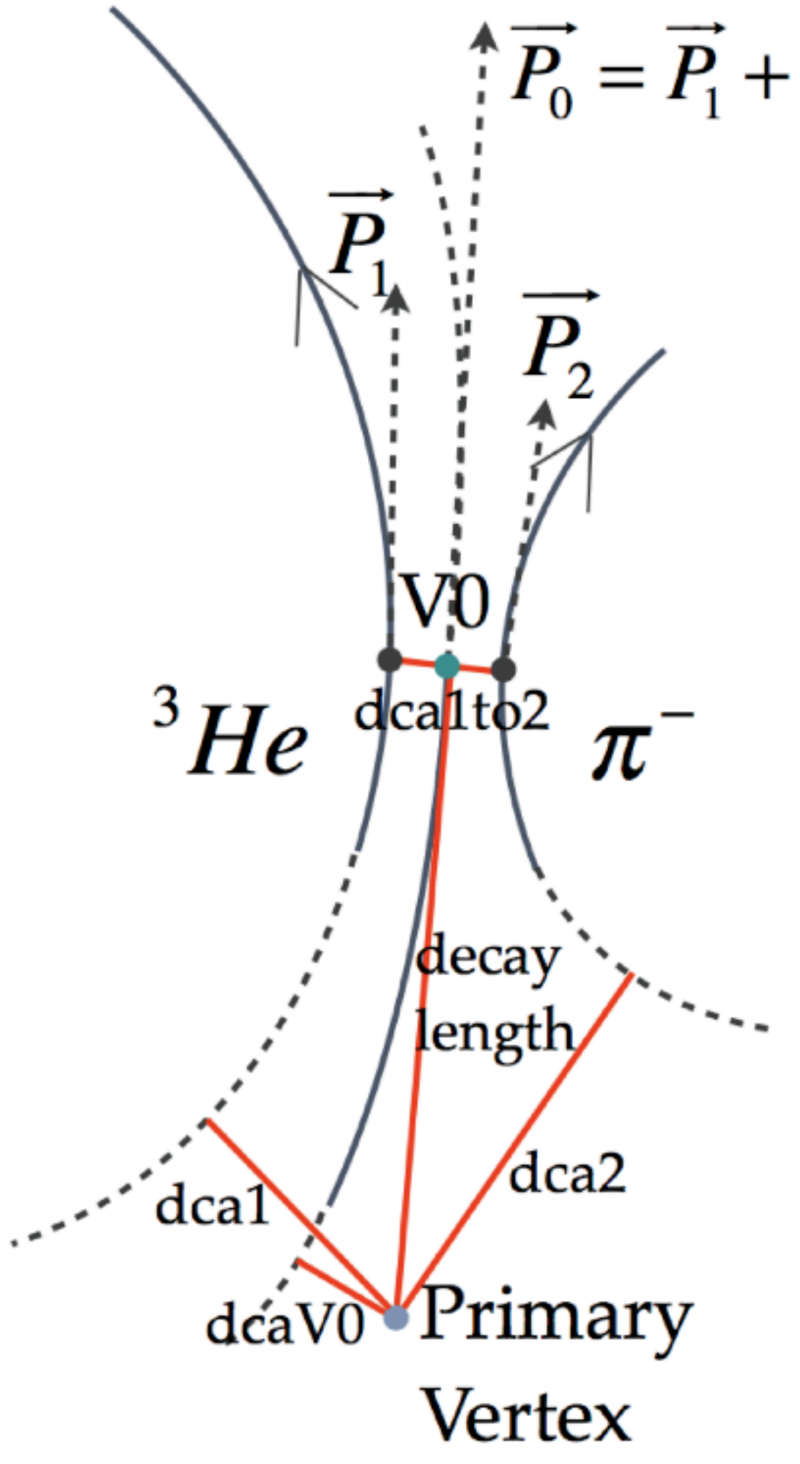

- Particle identification from energy loss measurement using TPC
- KF particle package[1] is used for signal reconstruction
- Hypernuclei reconstructed via their weak decay channels:

$^{3}_{\Lambda}\mathrm{H}\rightarrow {}^{3}\mathrm{He}+\pi^{-}$ $^{3}_{\Lambda}\mathrm{H}\rightarrow \mathrm{d}+\mathrm{p}+\pi^{-}$ $^{4}_{\Lambda}\mathrm{H}\rightarrow {}^{4}\mathrm{He}+\pi^{-}$ $^{4}_{\Lambda}\mathrm{He}\rightarrow {}^{3}\mathrm{He}+\mathrm{p}+\pi^{-}$

[1] Zyzak M, Kisel I, Senger P. Online selection of short-lived particles on many-core computer architectures in the CBM experiment at FAIR[R]. Collaboration FAIR: CBM, 2016.

Hypernuclei signal reconstruction

2-body decay channels: STAR, PRL 128, 202301(2022)

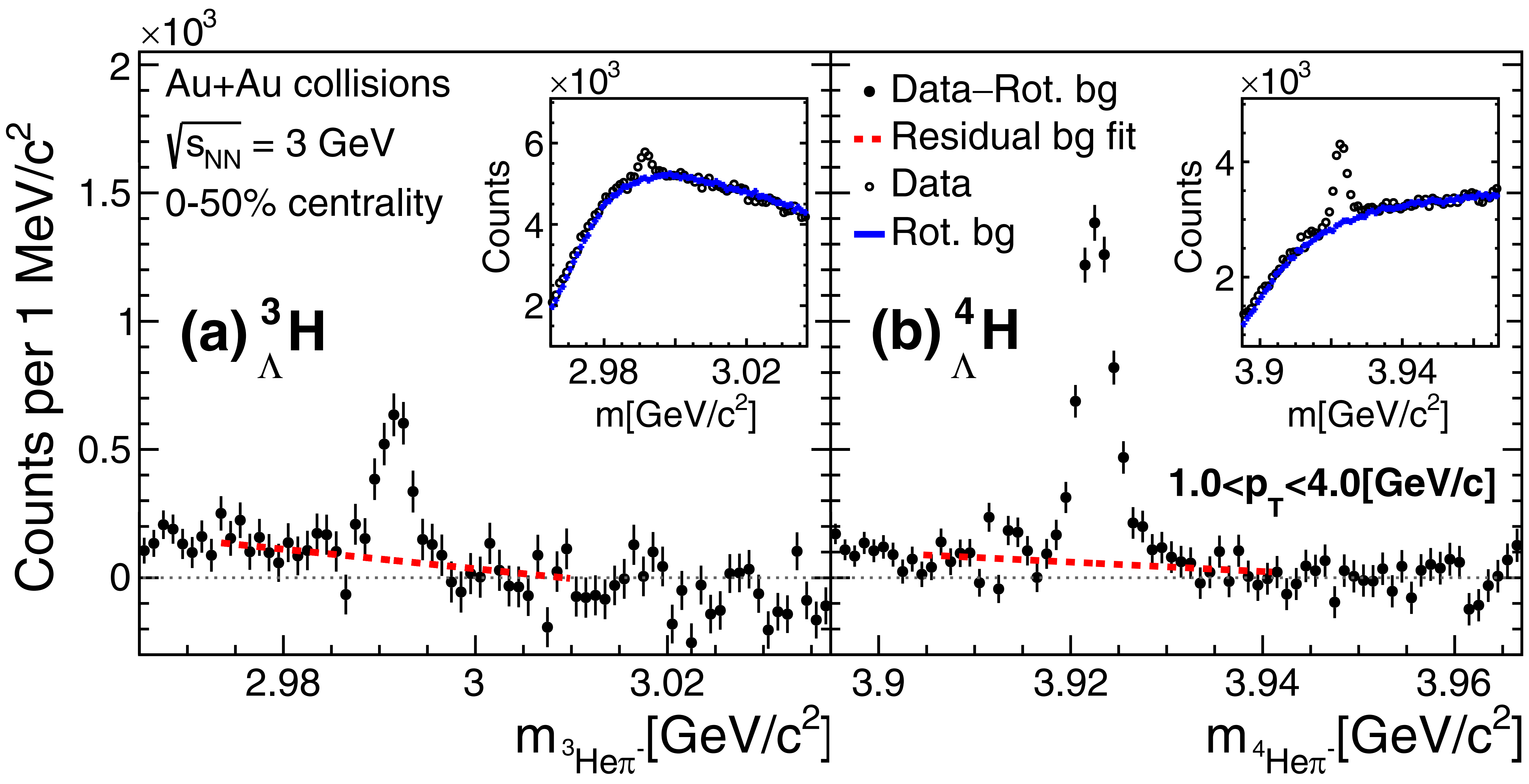

3-body decay channels:

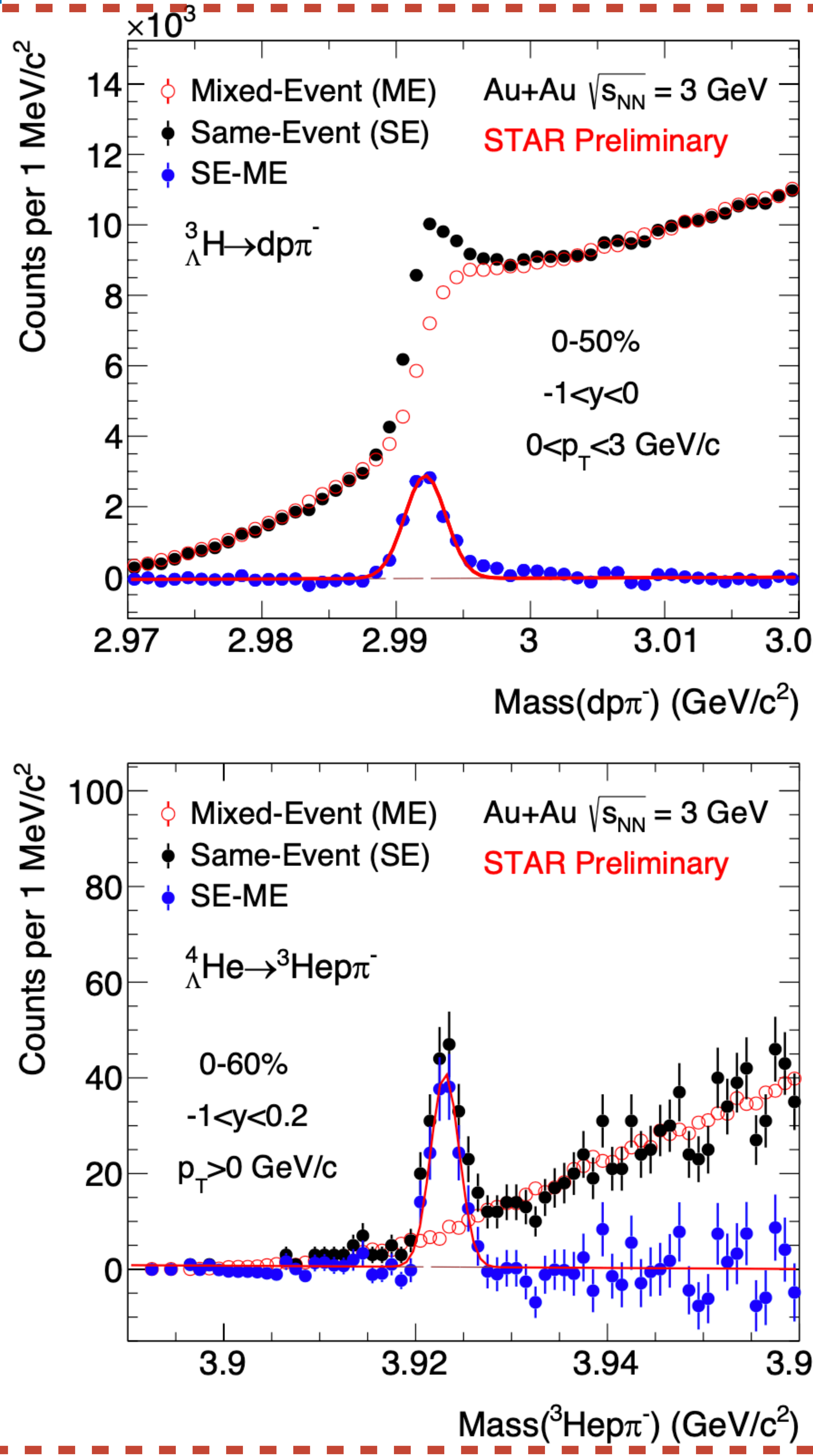

- Combinatorial background estimated via:
  - Rotating pion tracks for 2-body decay channels here
  - Event mixing for 3-body decay channels here

${}^{3}_{\Lambda}\mathrm{H}$ branching ratio R_3

Relative branching ratio: $\mathrm{R}_3 = \dfrac{\mathrm{B.R.}({}^{3}_{\Lambda}\mathrm{H} \to {}^{3}\mathrm{He}\pi^-)}{\mathrm{B.R.}({}^{3}_{\Lambda}\mathrm{H} \to {}^{3}\mathrm{He}\pi^-) + \mathrm{B.R.}({}^{3}_{\Lambda}\mathrm{H} \to \mathrm{d}p\pi^-)}$

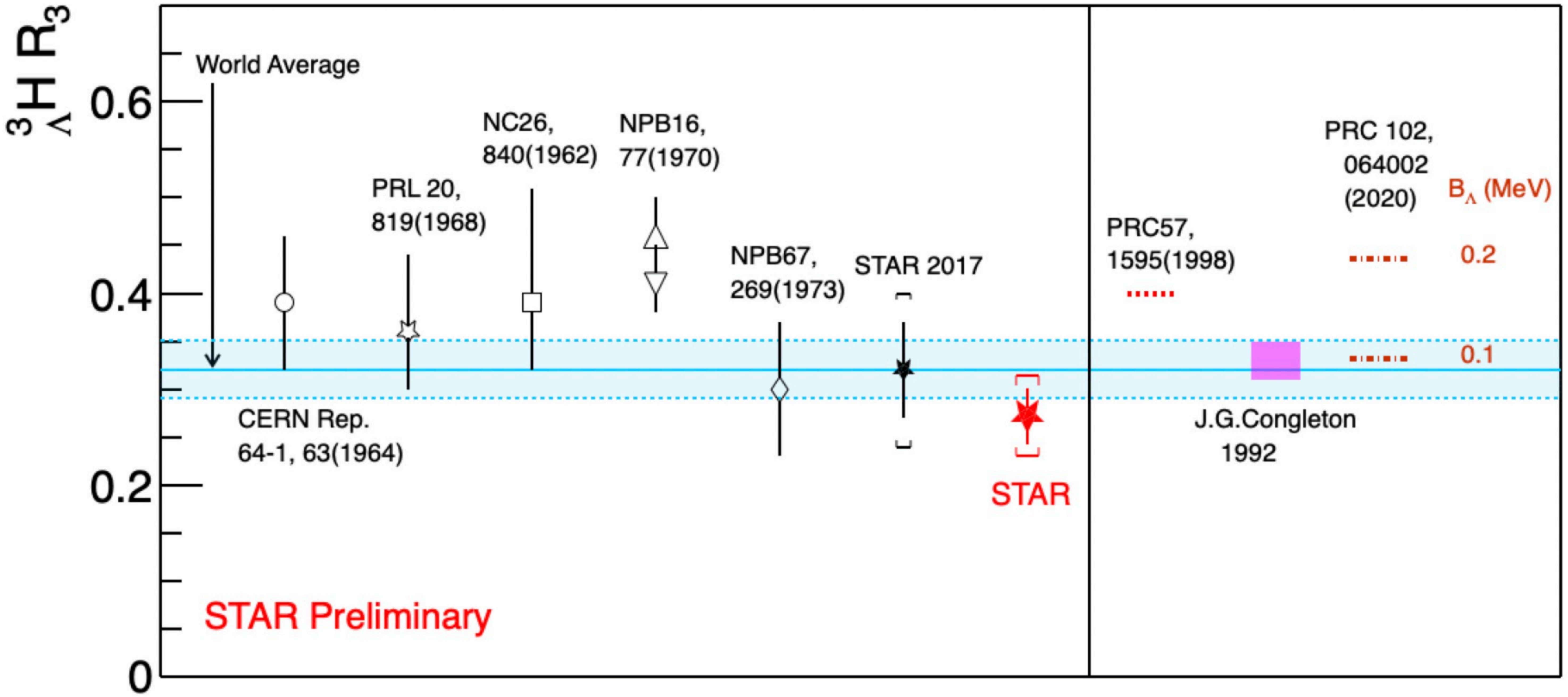

F. Hildenbrand et al. PRC 102, 064002 (2020)

- Recent calculation shows that R_3 may be sensitive to the binding energy (B_Λ) of ${}^{3}_{\Lambda}\mathrm{H}$
  - B_Λ → provide constraints to Y-N interaction

- Using $\sqrt{s_{NN}}$ = 3.0 GeV data:
  - $\mathrm{R}_3 = 0.272 \pm 0.030(\mathrm{stat.}) \pm 0.042(\mathrm{syst.})$
  - Model comparison suggesting a weakly-bounded state for ${}^{3}_{\Lambda}\mathrm{H}$

- Improved precision on R_3
  - Stronger constraints on absolute B.R.s and ${}^{3}_{\Lambda}\mathrm{H}$ internal structure models

$^{3}_{\Lambda}\mathrm{H}$, $^{4}_{\Lambda}\mathrm{H}$ and $^{4}_{\Lambda}\mathrm{He}$ lifetimes

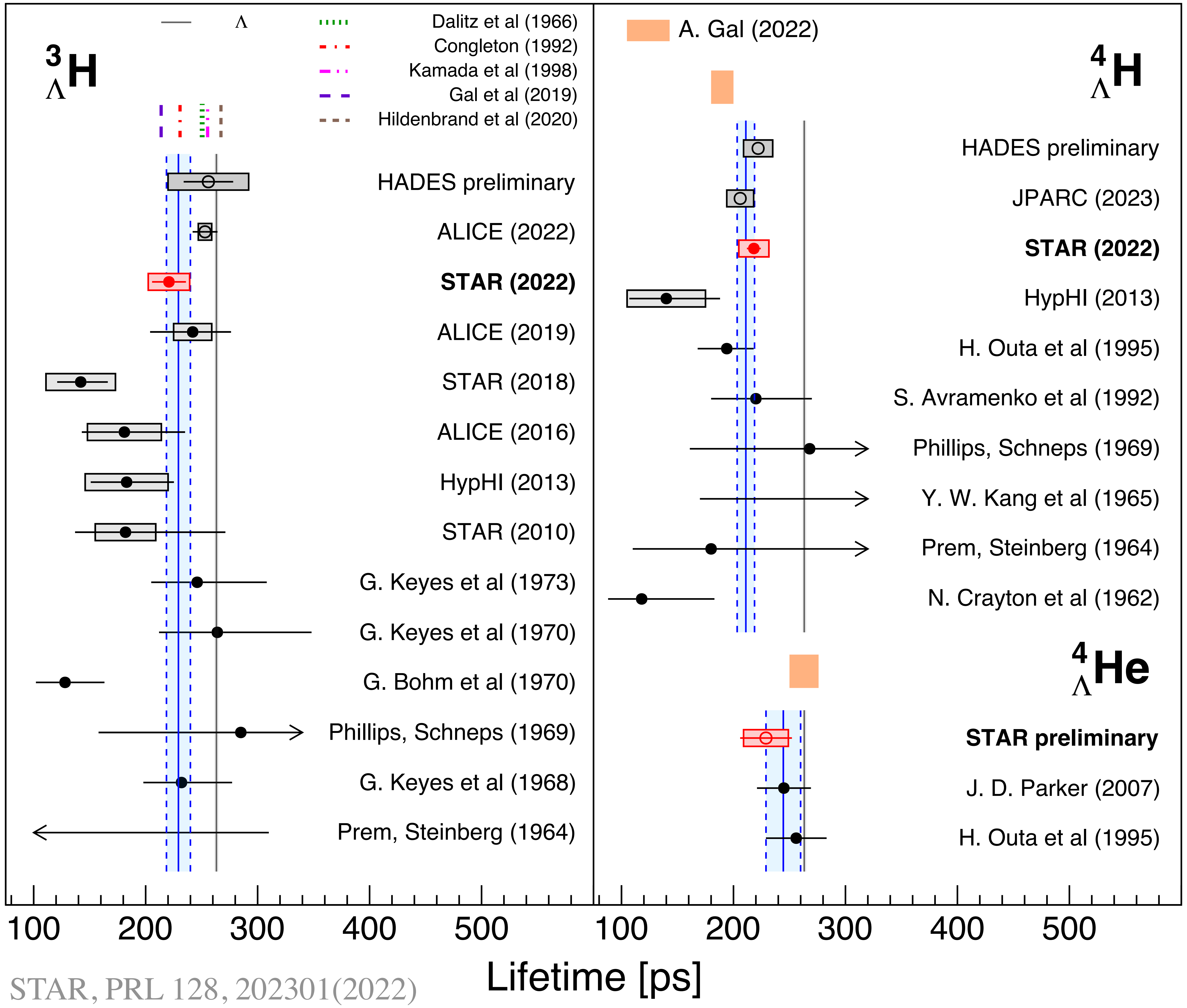

STAR, PRL 128, 202301(2022)

$^{3}_{\Lambda}$H: ALICE(2022),arXiv:2209.07360

$^{4}_{\Lambda}$H: JPARC(2023),arXiv:2302.07443

Using $\sqrt{s_{NN}}$ = 3.0 GeV and 7.2 GeV datasets:

$^{3}_{\Lambda}\mathrm{H}$: $\tau = 221 \pm 15(\mathrm{stat.}) \pm 19(\mathrm{syst.})[\mathrm{ps}]$

$^{4}_{\Lambda}\mathrm{H}$: $\tau = 218 \pm 6(\mathrm{stat.}) \pm 13(\mathrm{syst.})[\mathrm{ps}]$

$^{4}_{\Lambda}\mathrm{He}$: $\tau = 229 \pm 23(\mathrm{stat.}) \pm 20(\mathrm{syst.})[\mathrm{ps}]$

- Indication of shorter lifetimes for $^{3}_{\Lambda}\mathrm{H}$, $^{4}_{\Lambda}\mathrm{H}$ and $^{4}_{\Lambda}\mathrm{He}$ than that of free Λ (with 1.8σ, 3.0σ, 1.1σ respectively)
- Consistent with former measurements and world average values
- $\tau_{^{3}_{\Lambda}\mathrm{H}}$: consistent with calculation including pion FSI[1] and calculation with Λd 2-body picture[2] within 1σ
- $\tau_{^{4}_{\Lambda}\mathrm{H}}$ and $\tau_{^{4}_{\Lambda}\mathrm{He}}$: consistent with expectations from isospin rule

Precision $^{3}_{\Lambda}\mathrm{H}$ and $^{4}_{\Lambda}\mathrm{H}$ measurements provide tighter constraints on models.

[1] A. Gal and H. Garcilazo, PLB 791, 48 (2019)
[2] J.G. Congleton, J. Phys. G 18, 339 (1992)

Hypernuclei production at 3 GeV

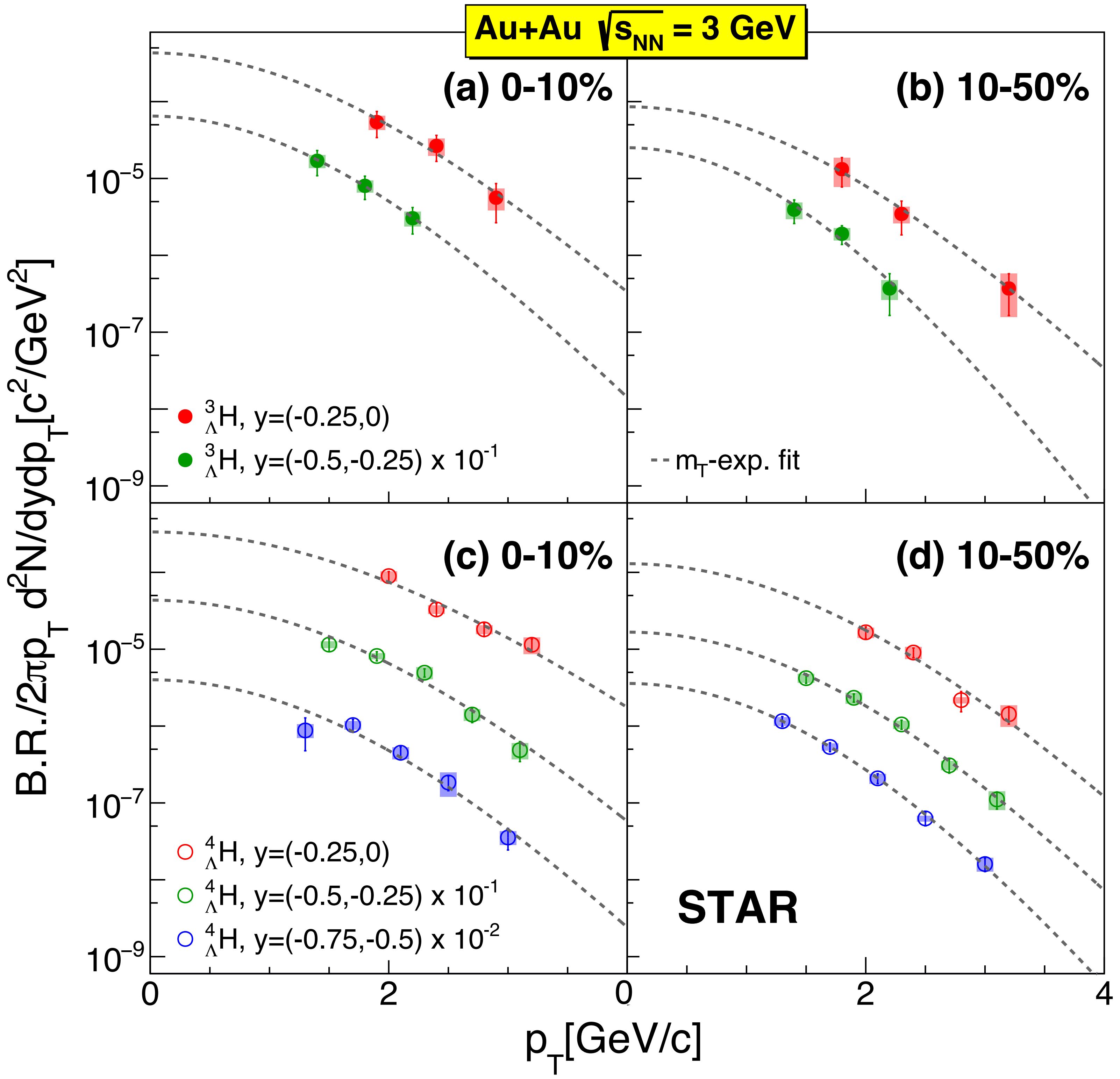

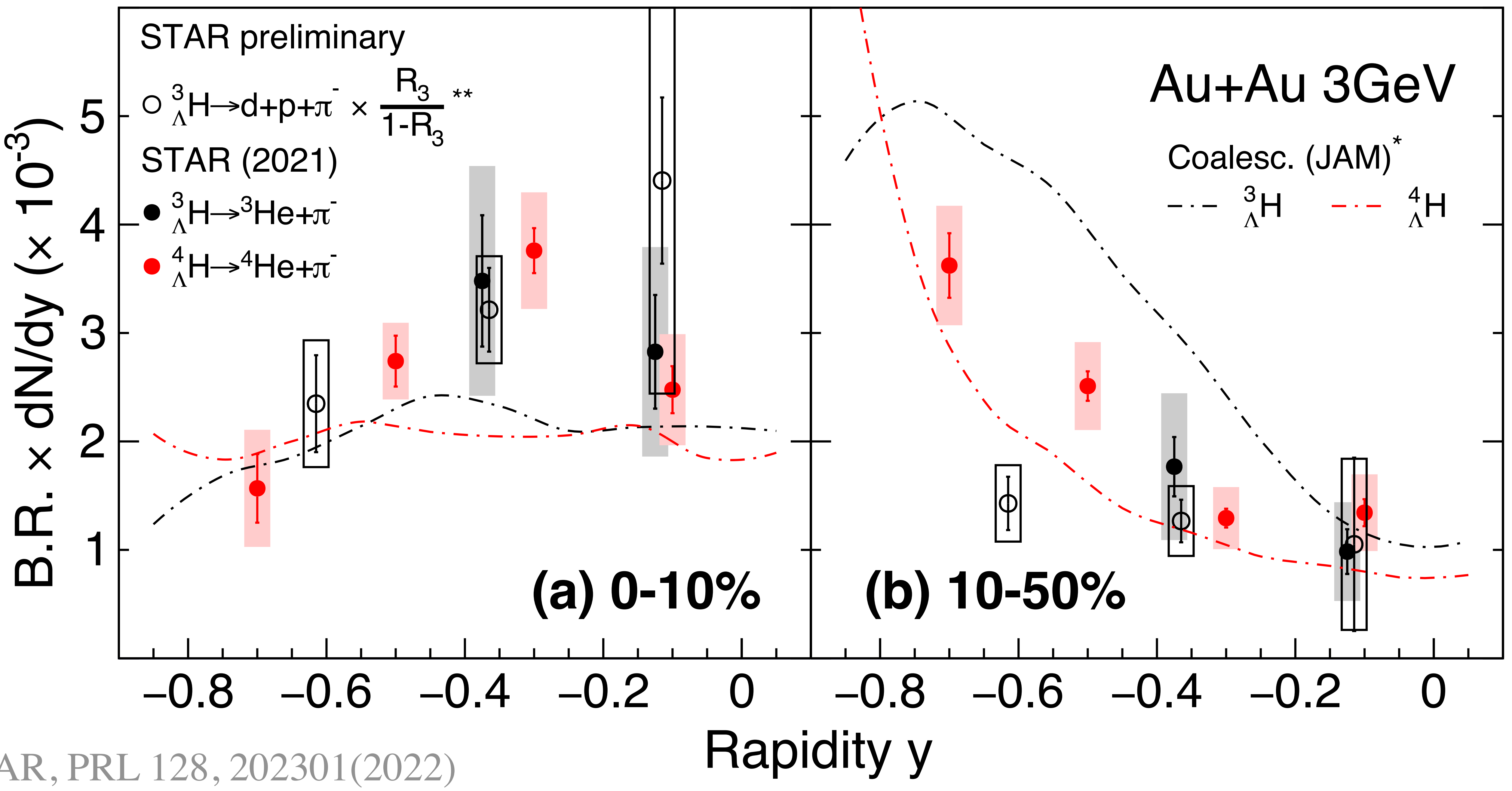

STAR, PRL 128, 202301(2022)

- Different trends in the ${}^4_\Lambda$H rapidity distribution in central (0-10%) and mid-central (10-50%) collisions at $\sqrt{s_{NN}}$ = 3.0 GeV
  - Transport model (JAM) with coalescence approximately reproduces trends of ${}^4_\Lambda$H rapidity distributions seen in data, but fails to reproduce the trend of ${}^3_\Lambda$H in 10-50%

${}^{3}_{\Lambda}\mathrm{H}$ and ${}^{4}_{\Lambda}\mathrm{H}$ directed flow at 3 GeV

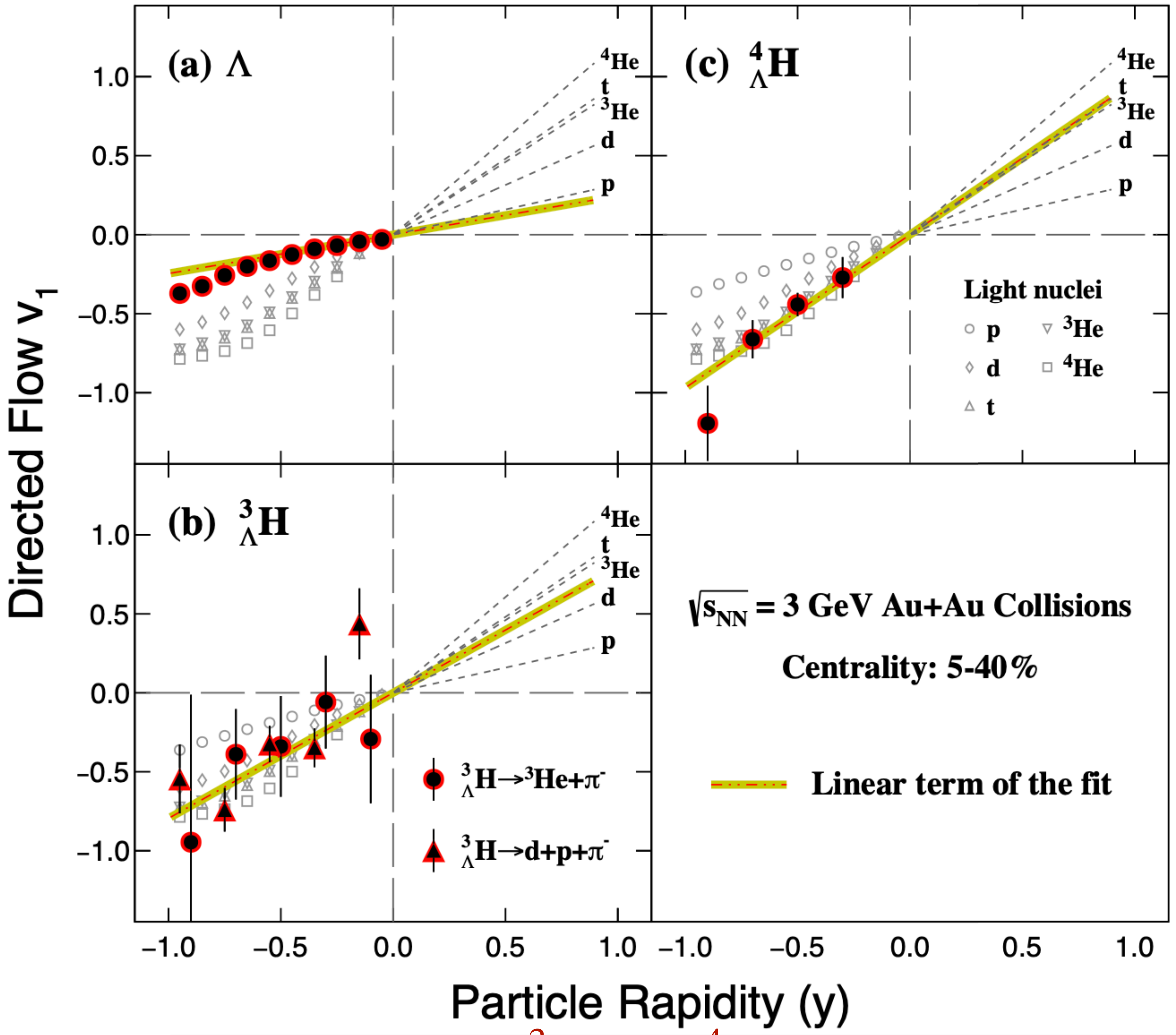

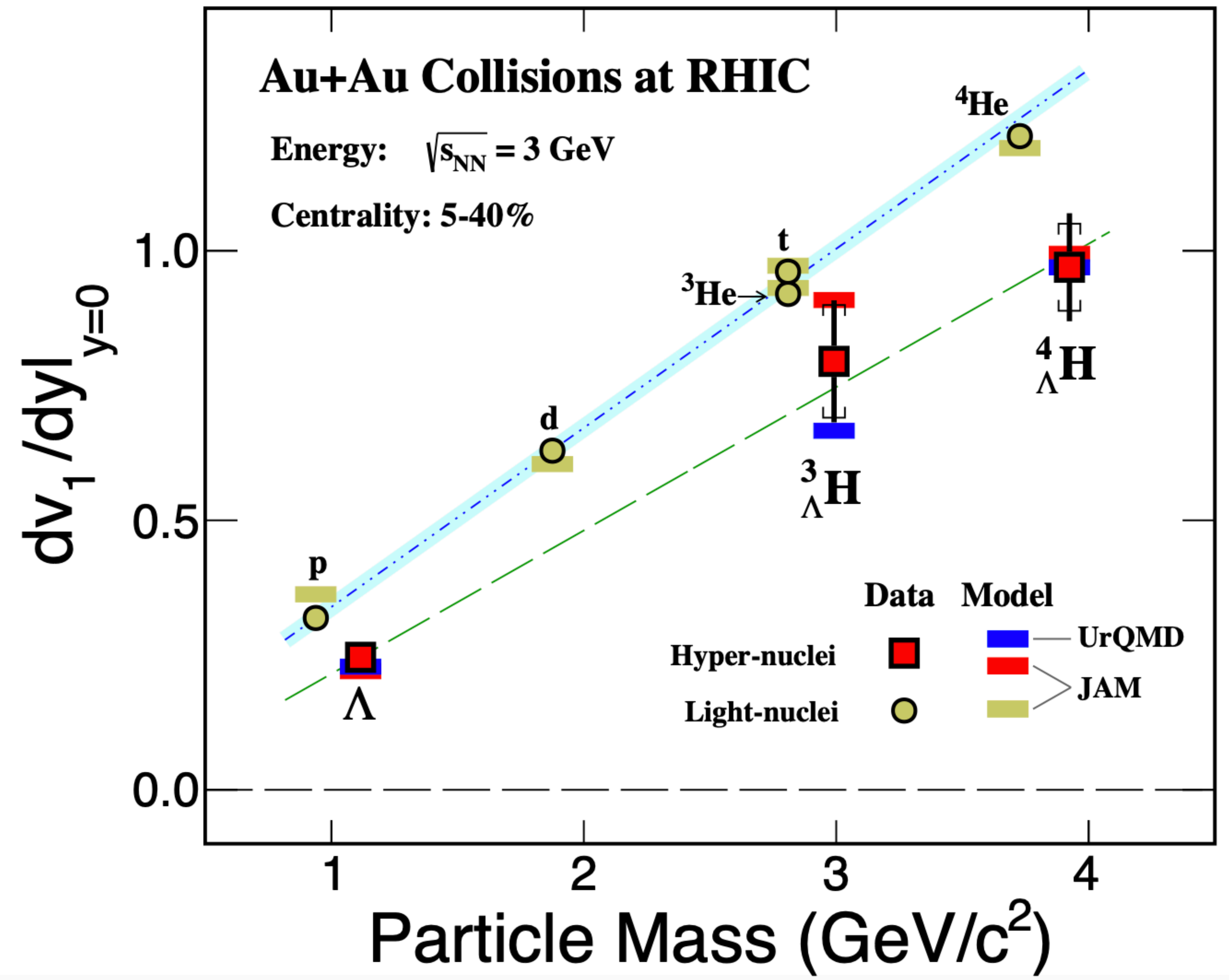

arXiv:2211.16981
accepted by PRL

- First observation of ${}^{3}_{\Lambda}\mathrm{H}$ and ${}^{4}_{\Lambda}\mathrm{H}$ directed flow (v_1) in mid-central 5-40% Au+Au collisions at 3 GeV
- Mid-rapidity v_1 slopes of ${}^{3}_{\Lambda}\mathrm{H}$ and ${}^{4}_{\Lambda}\mathrm{H}$ follow baryon mass scaling.

→ Imply coalescence process to be the dominant formation mechanism for ${}^{3}_{\Lambda}\mathrm{H}$ and ${}^{4}_{\Lambda}\mathrm{H}$ production in the 3 GeV heavy-ion collisions

Energy dependence of hypernuclei production in heavy-ion collisions

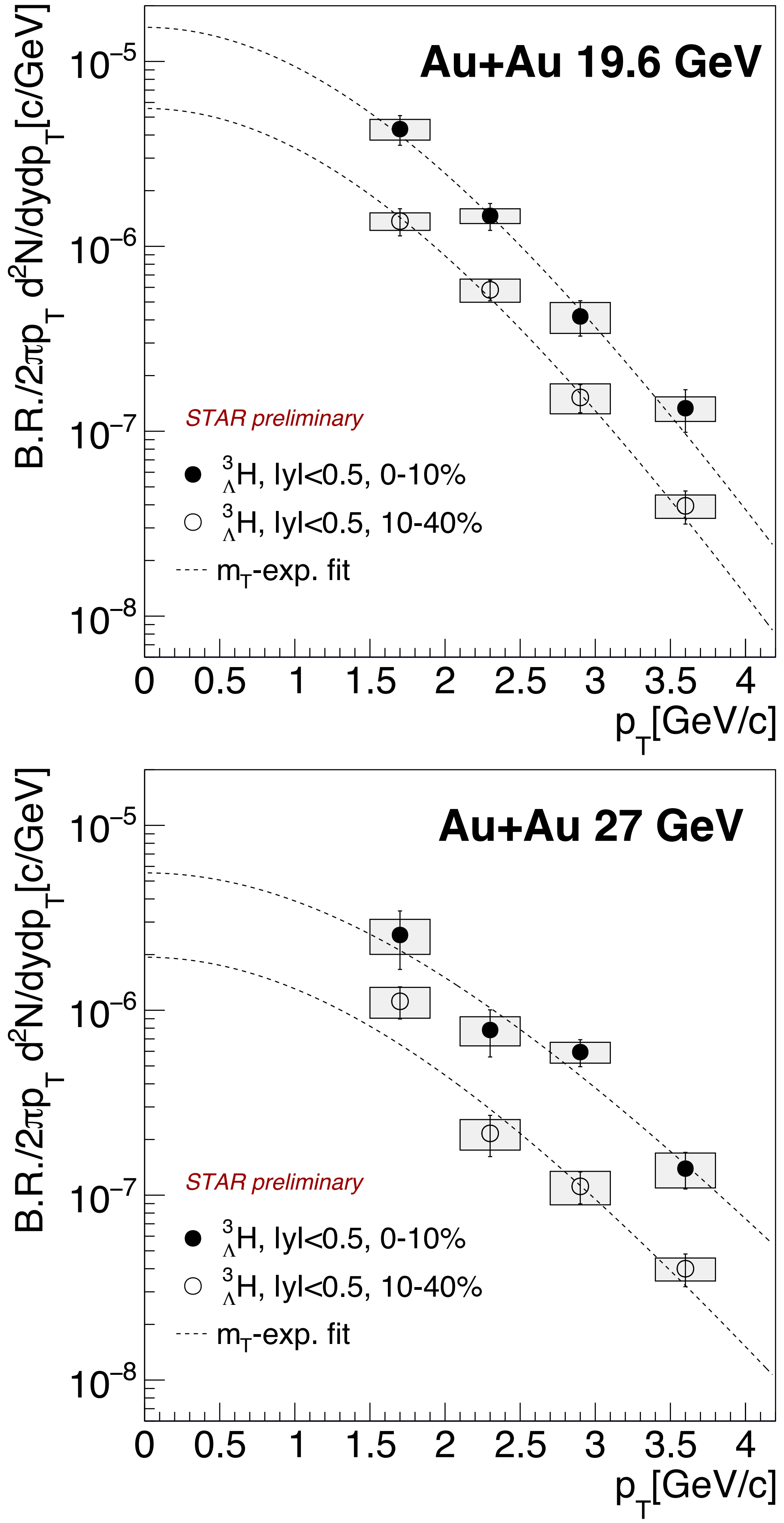

- ${}^{3}_{\Lambda}\mathrm{H}$ mid-rapidity yields obtained as a function of p_T and centrality at 19.6 and 27 GeV

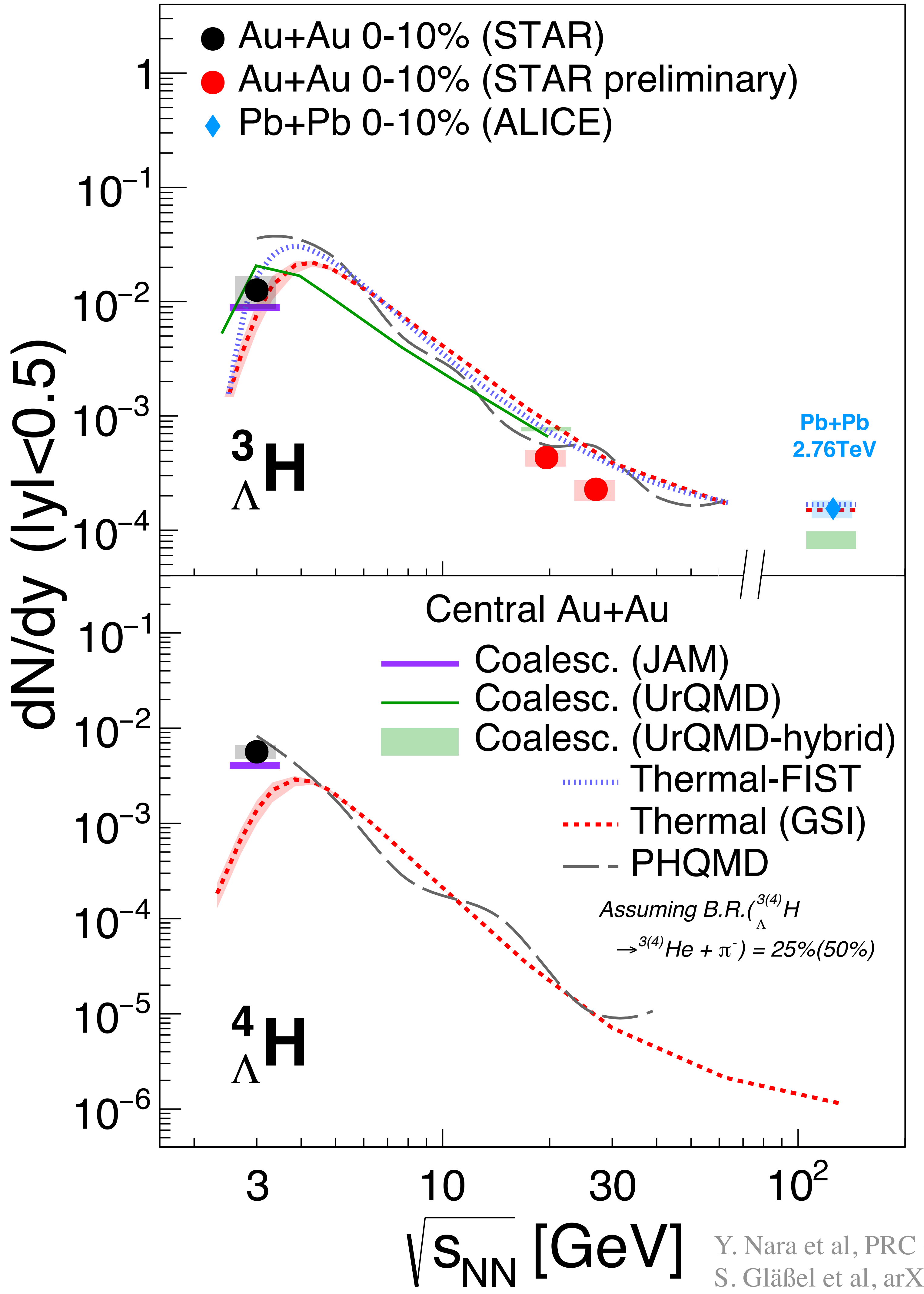

STAR, PRL 128 (2022) 202301
ALICE, PLB 754 (2016) 360

Y. Nara et al, PRC 61 (1999) 024901 (JAM)
S. Gläßel et al, arXiv: 2106,14839 (PHQMD)
A. Andronic et al, PLB 697 (2011) 203 (Thermal (GSI))
T. Reichert, J. Steinheimer et al, arXiv:2210.11876(2022) (UrQMD, Thermal-FIST)

- ${}^{3}_{\Lambda}\mathrm{H}$ yield at mid-rapidity increases from 2.76 TeV to 3 GeV
  - Driven by increase in baryon density at low energies
- Thermal(GSI), Coalescence(UrQMD), Thermal-FIST and PHQMD reproduce the trend

For Au+Au @ 3 GeV

- Coalescence(JAM) with tuned parameters can describe data
- PHQMD describes ${}^{4}_{\Lambda}\mathrm{H}$, but overestimates ${}^{3}_{\Lambda}\mathrm{H}$

Provide first constraints for hypernuclei production models in the high-baryon-density region

Hyper-to-light nuclei ratios

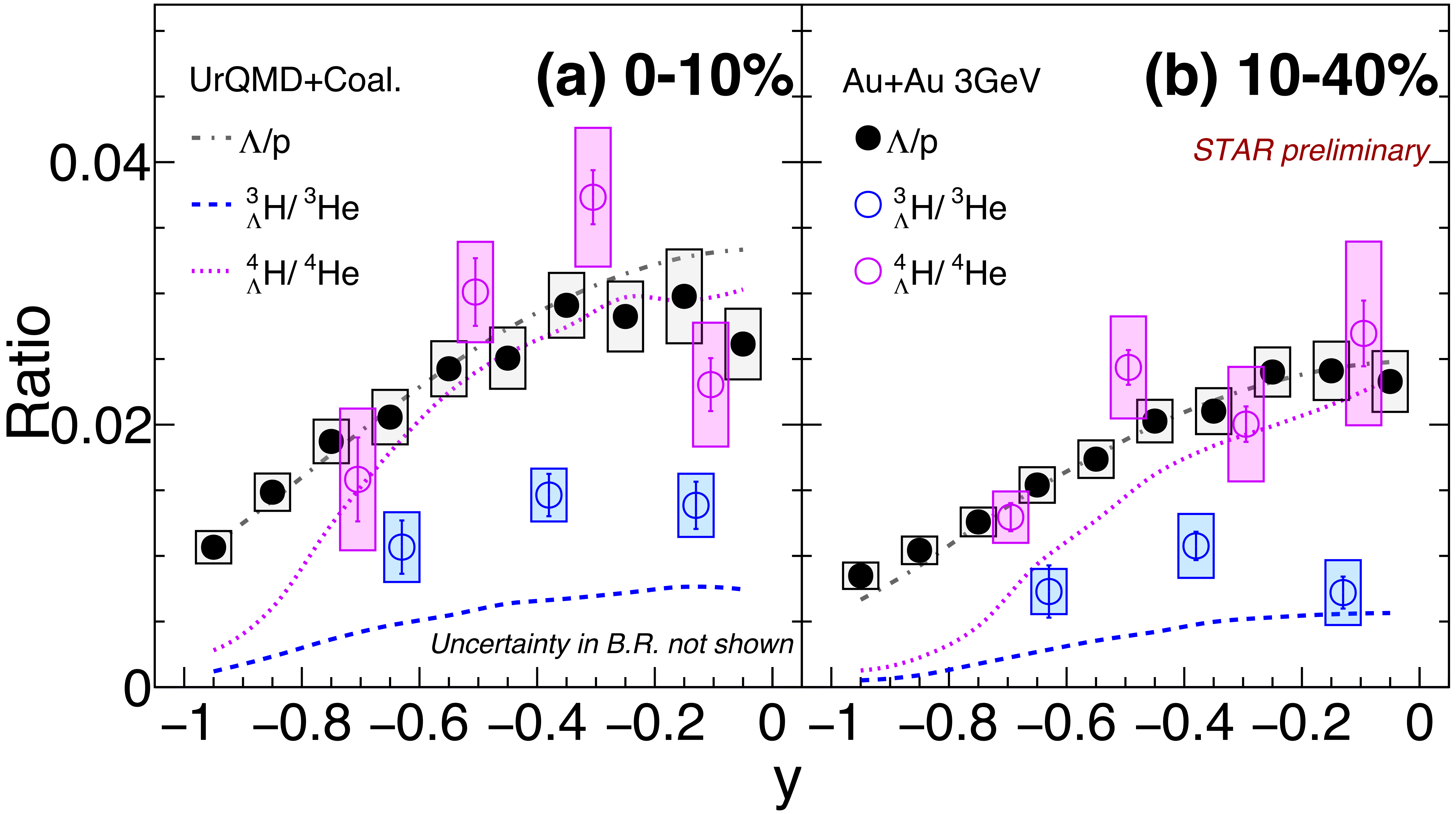

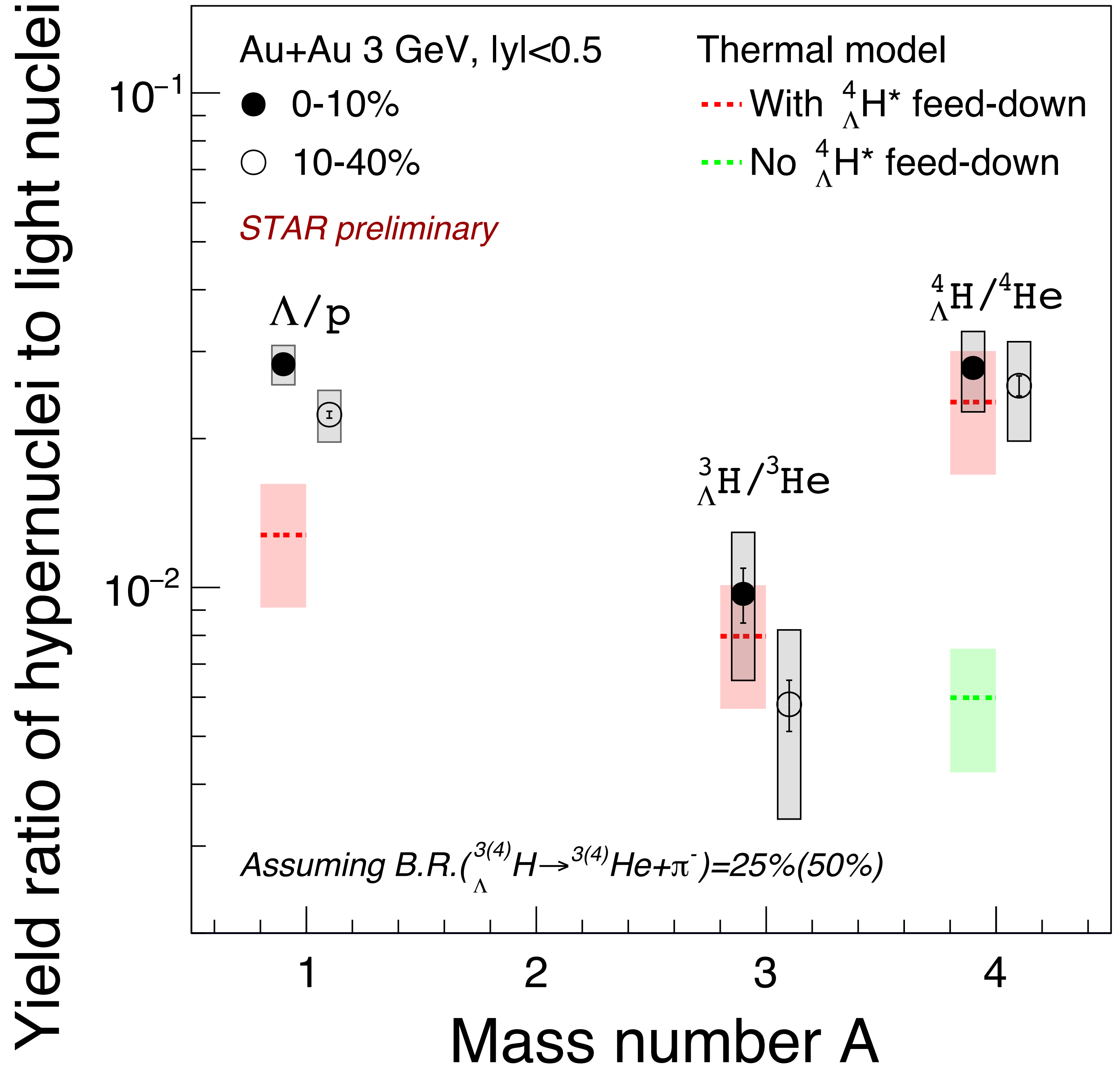

A. Andronic et al, PLB 697 (2011) 203 (Thermal model)

- **Suppression of $^3_\Lambda\mathrm{H}/^3\mathrm{He}$ yield ratios compared to that of Λ/p**
  - Observed at both 0-10% and 10-40% centrality in Au+Au collisions at 3 GeV.
- **The $^4_\Lambda\mathrm{H}/^4\mathrm{He}$ yield ratios are comparable to that of Λ/p**
- **UrQMD model with coalescence describes the tendency of the distributions reasonably well, suggesting coalescence mechanism for hypernuclei formation.**

- **Non-monotonic behavior in light-to-hyper-nuclei ratio vs A**
- **Thermal model calculations including excited $^4_\Lambda\mathrm{H}^*$ feed-down show a similar trend**
  - Feed-down from excited state enhances $^4_\Lambda\mathrm{H}$ production

Suggest coalescence mechanism and creation of excited A = 4 hypernuclei

$S_{3,4}$ at 3 GeV

- **Strangeness population factor S_A**
  - Relative suppression of hypernuclei production compared to light nuclei production

$$S_A = \frac{{}^{A}_{\Lambda}\mathrm{H}}{{}^{A}\mathrm{He} \times \frac{\Lambda}{p}} = \frac{B_A({}^{A}_{\Lambda}\mathrm{H})(p_T)}{B_A({}^{A}\mathrm{He})(p_T)}$$

S.Zhang, PLB 684(2010)224

- B_A: Coalescence parameters

  - Expect ~1 if no suppression

$S_3 < 1$: relative suppression of ${}^{3}_{\Lambda}\mathrm{H}/{}^{3}\mathrm{He}$ compared to Λ/p

$S_4 \sim 1$, $S_4 > S_3$: ${}^{4}_{\Lambda}\mathrm{H}/{}^{4}\mathrm{He}$ is comparable to Λ/p

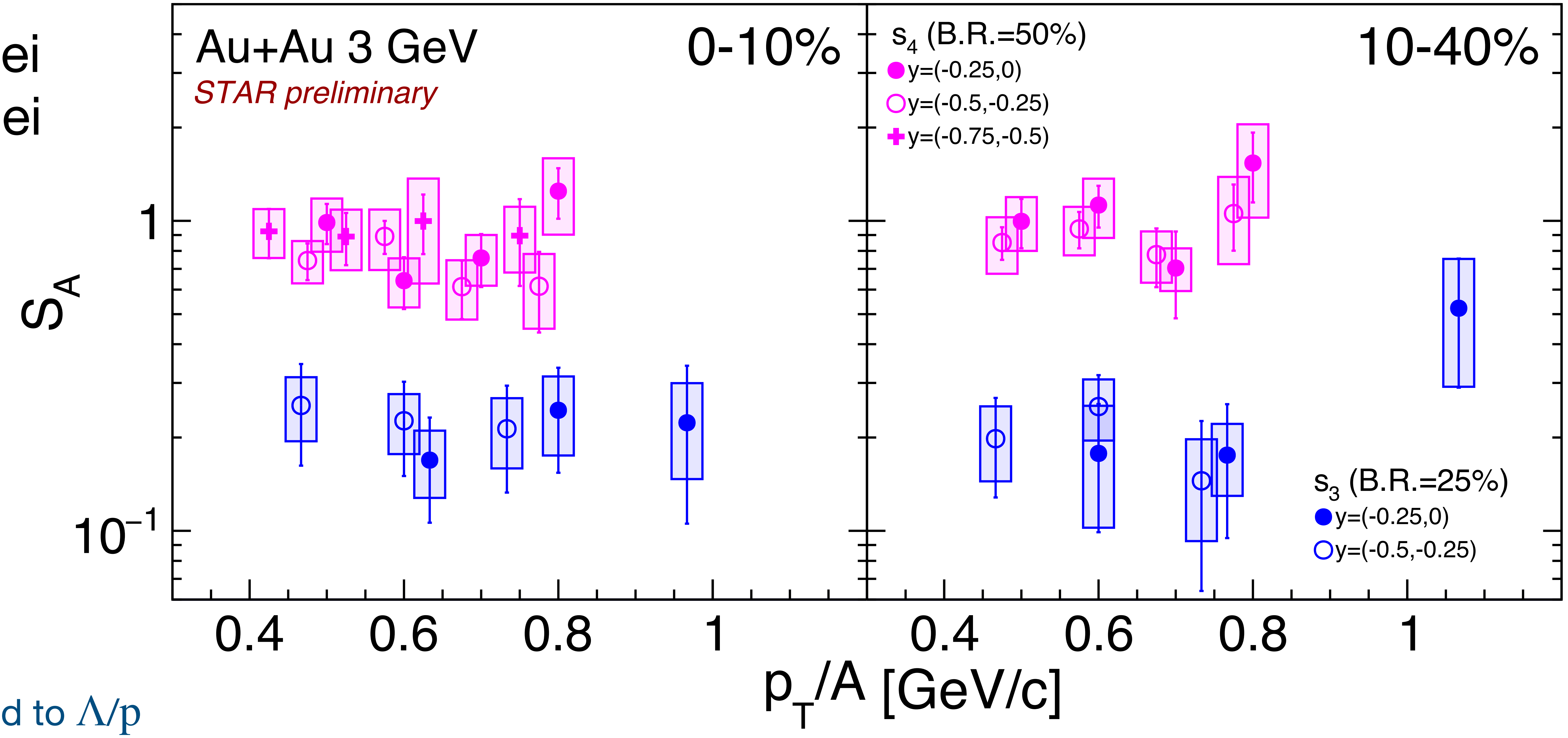

No obvious kinematic and centrality dependence of $S_{3,4}$ is observed at 3 GeV.

→ Coalescence parameter B_A of ${}^{A}_{\Lambda}\mathrm{H}$ and ${}^{A}\mathrm{He}$ follows similar tendency versus p_T, rapidity and centrality, indicates that N-N and Y-N interactions that drive coalescence dynamics in these collisions are similar

Energy dependence of S_3

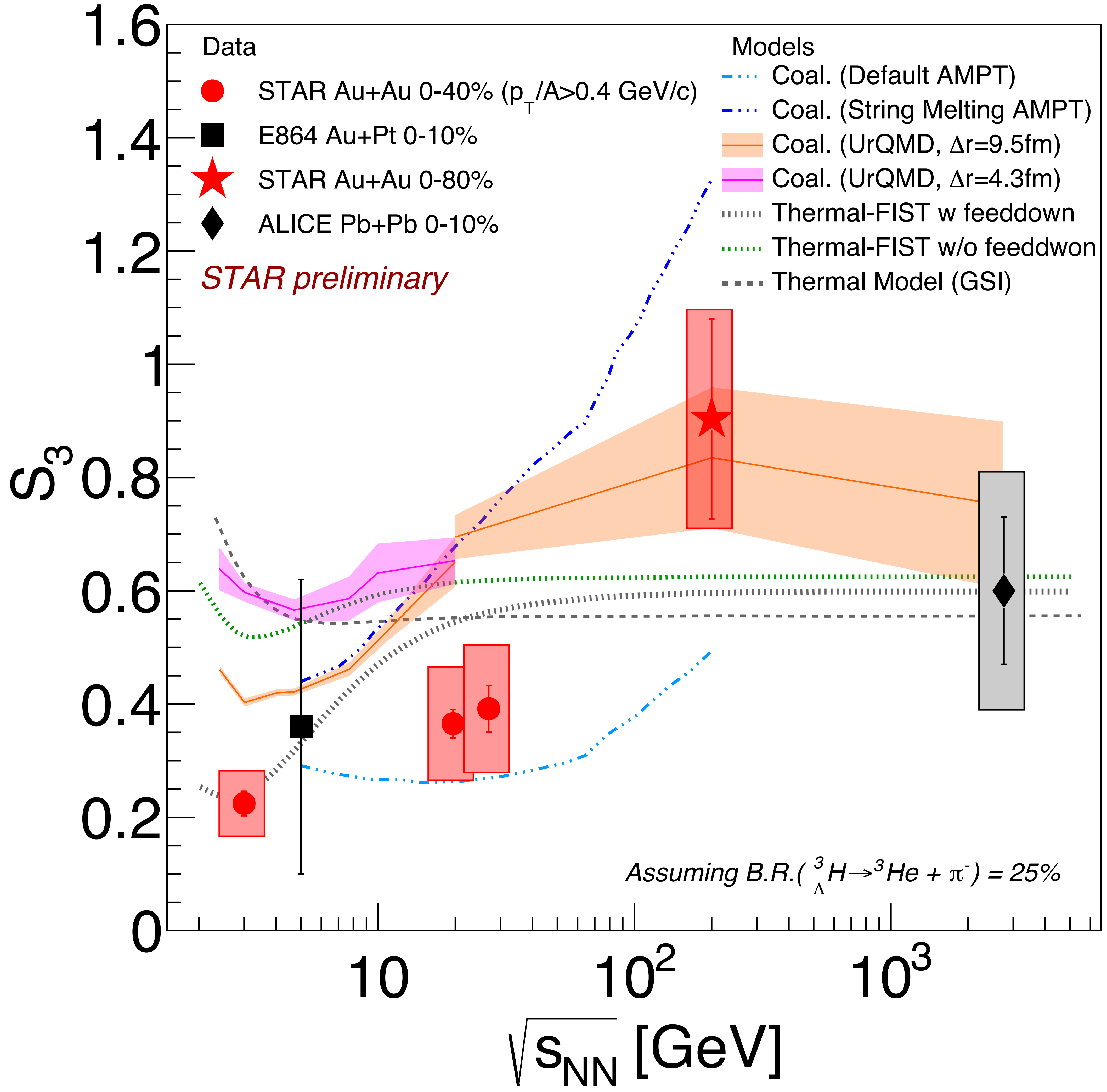

STAR, Science 328 (2010) 58
ALICE, PLB 754 (2016) 360
E864, PRC 70 (2004) 024902
NA49, J.Phys.Conf.Ser.110(2008)032010

A. Andronic et al, PLB 697 (2011) 203 (Thermal (GSI))
S. Zhang, PLB 684(2010)224 (Coal.+AMPT)
T. Reichert, J. Steinheimer et al, arXiv:2210.11876(2022) (UrQMD, Thermal-FIST)

- Data show a hint of an increasing trend from $\sqrt{s_{NN}}$ = 3.0 GeV to 2.76 TeV
- For coalescence models, the energy dependence is sensitive to the source radius (Δr)
- Thermal-FIST, which includes feed-down to p and ^{3}He from unstable nuclei, describes the S_3 data reasonably well

Provide constraints for hypernuclei production models in the high-baryon-density region

Summary

Presented measurements on hypernuclei production in the high-baryon-density region with high statistical precision using STAR data

- **Hypernuclei structure**
  - **Precision $^{3}_{\Lambda}\mathrm{H}$, $^{4}_{\Lambda}\mathrm{H}$ lifetimes and R_3 of $^{3}_{\Lambda}\mathrm{H}$ measured**
    - **Strong constraints on hyperon-nucleon interaction models**

- **Hypernuclei production in heavy-ion collisions**
  - **$^{3}_{\Lambda}\mathrm{H}$, $^{4}_{\Lambda}\mathrm{H}$ production yields at 3.0, 19.6 and 27 GeV**
    - Provide constraints to hypernuclei production models in the high-baryon-density region
    - Relative suppression of $^{3}_{\Lambda}\mathrm{H}/^{3}\mathrm{He}$ compared to Λ/p and $^{4}_{\Lambda}\mathrm{H}/^{4}\mathrm{He}$; suggest coalescence formation of hypernuclei; suggest creation of $^{4}_{\Lambda}\mathrm{H}^{*}$
    - S_3 and S_4 show weak centrality/kinematic dependence; hint of increasing trend of S_3 vs $\sqrt{s_{\mathrm{NN}}}$
  - **$^{3}_{\Lambda}\mathrm{H}$ and $^{4}_{\Lambda}\mathrm{H}$ collectivity v_1**
    - v_1 slopes follow baryon mass scaling → Support coalescence picture

Outlook

1. iTPC and eToF fully installed in 2019 → extend η acceptance and improve PID at large η
2. High statistics data in STAR BES-II $\sqrt{s_{NN}}$ = 3.0 - 54.4 GeV, especially the **2 billion events** collected at 3 GeV in 2021 → larger statistics, higher precision

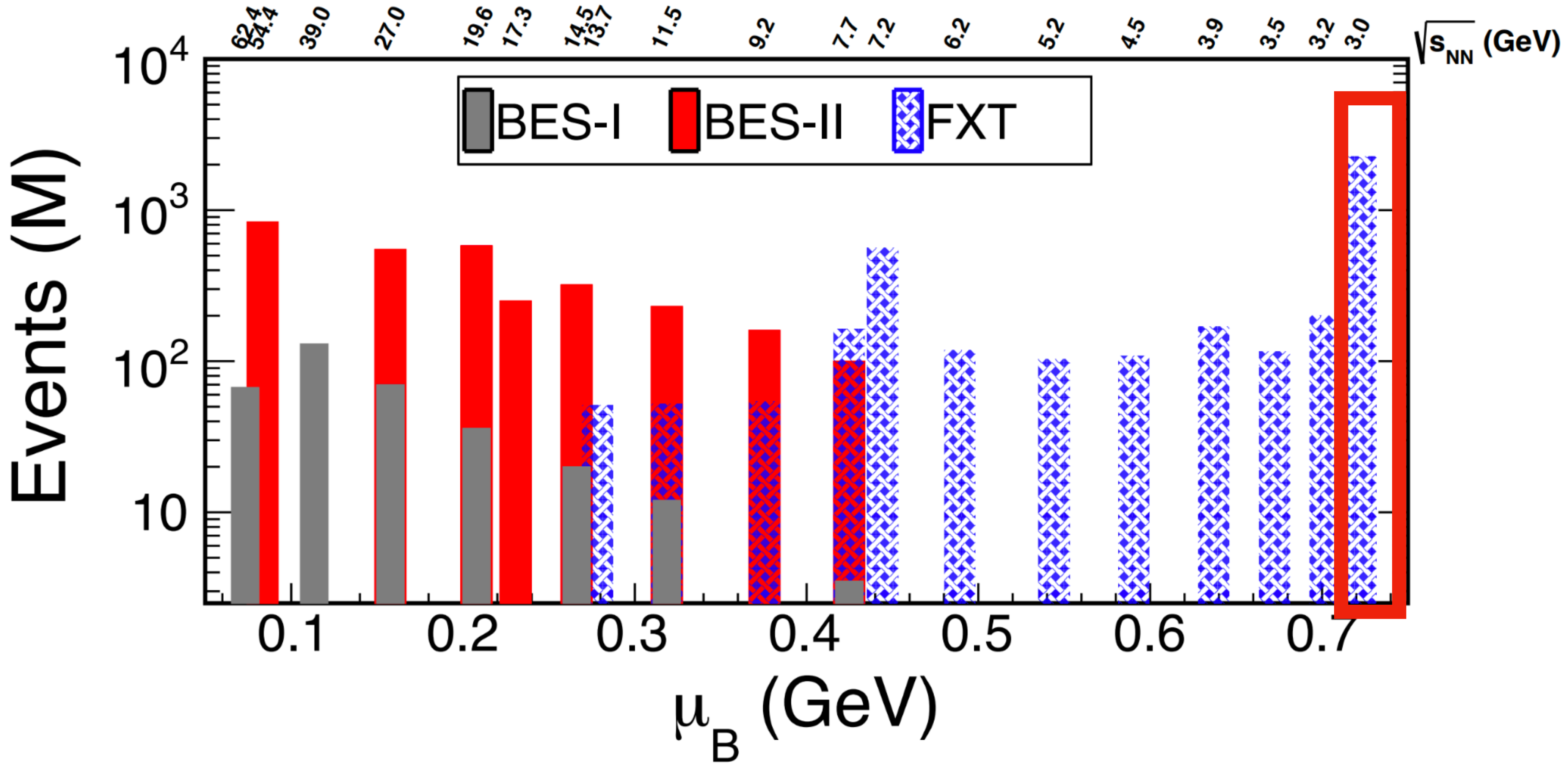

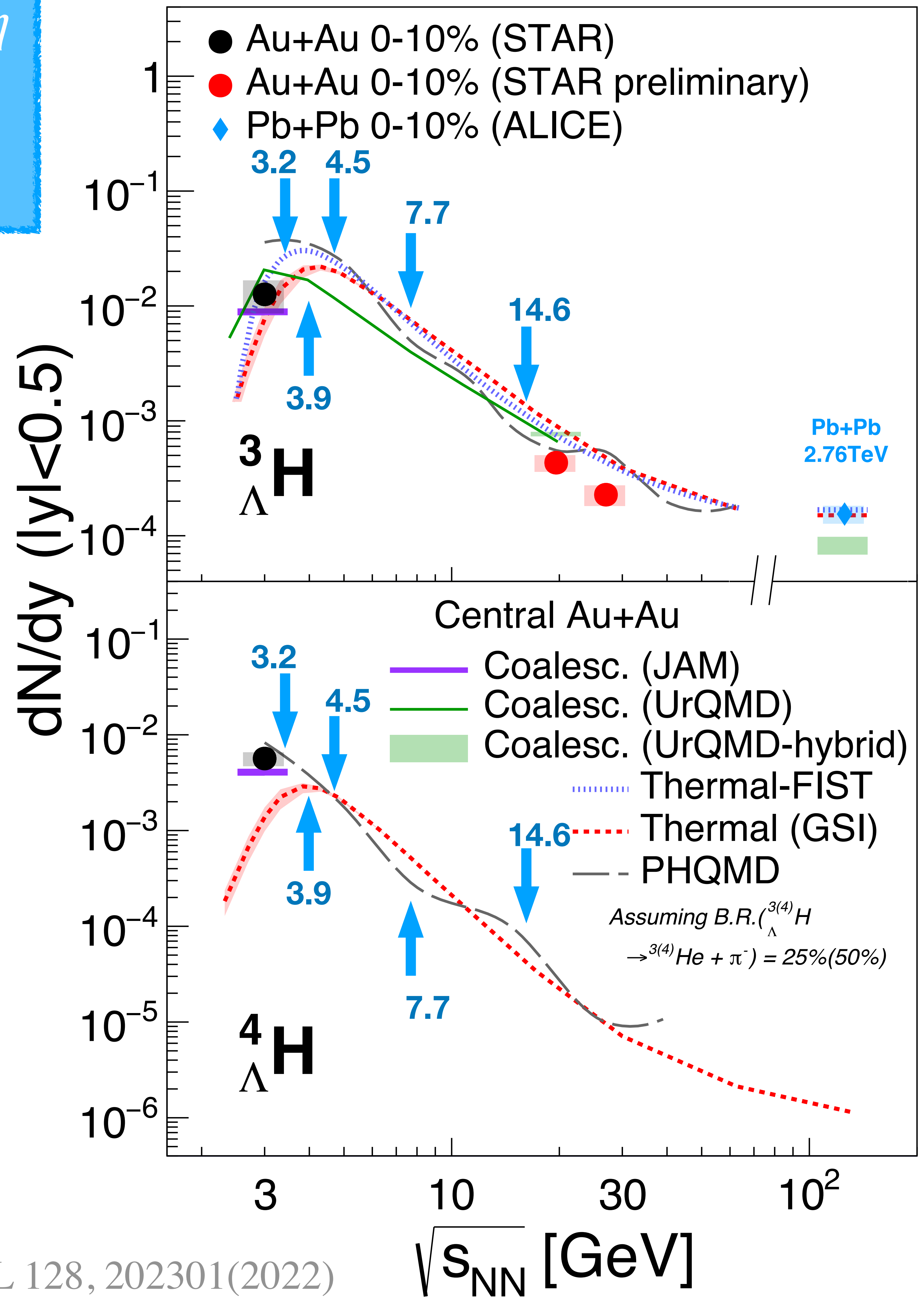

STAR, PRL 128, 202301(2022)

- Precision measurements on hypernuclei properties
- Energy dependence study of hypernuclei yields
- Search for double Λ hypernuclei
  - e.g. ${}^{4}_{\Lambda\Lambda}\mathrm{He} \rightarrow {}^{4}_{\Lambda}\mathrm{He}\pi$, ${}^{5}_{\Lambda\Lambda}\mathrm{He} \rightarrow {}^{5}_{\Lambda}\mathrm{He}\pi$

Outlook

1. iTPC and eToF fully installed in 2019 → extend η acceptance and improve PID at large η
2. High statistics data in STAR BES-II $\sqrt{s_{NN}}$ = 3.0 - 54.4 GeV, especially the **2 billion events** collected at 3 GeV in 2021 → larger statistics, higher precision

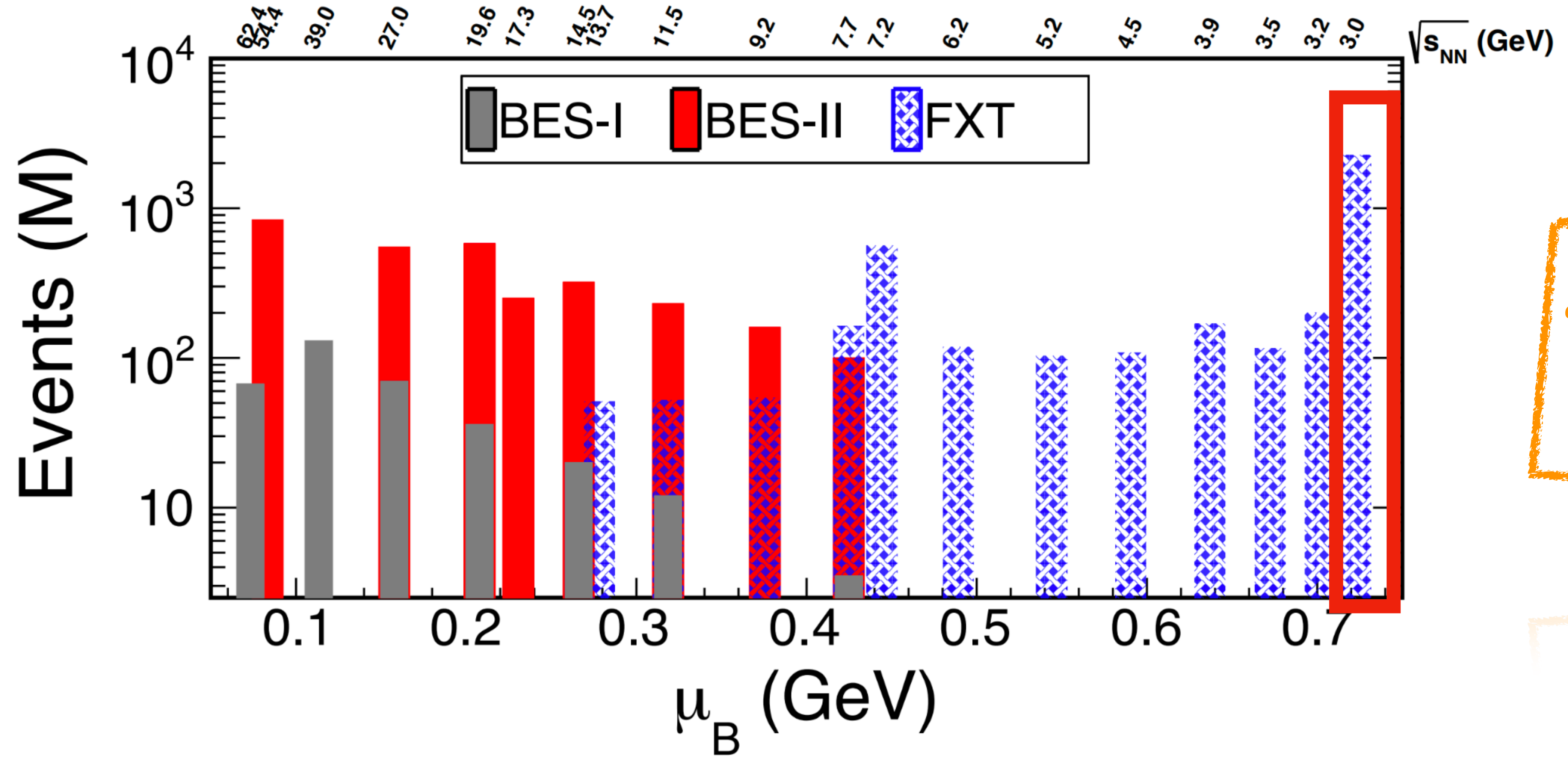

Thank you!

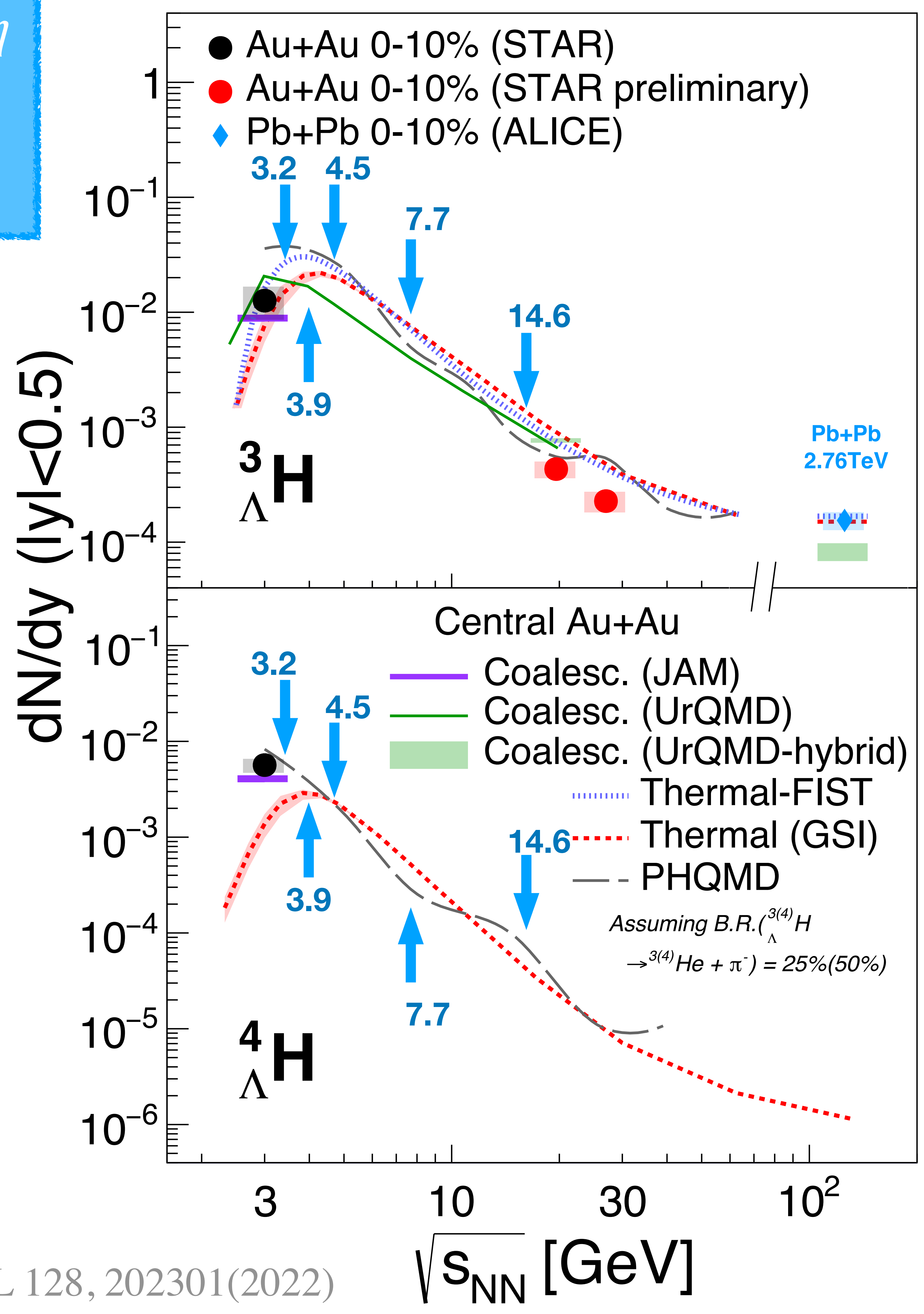

STAR, PRL 128, 202301(2022)

- Precision measurements on hypernuclei properties
- Energy dependence study of hypernuclei yields
- Search for double Λ hypernuclei
  - e.g. ${}^{4}_{\Lambda\Lambda}\mathrm{He} \rightarrow {}^{4}_{\Lambda}\mathrm{He}\pi$, ${}^{5}_{\Lambda\Lambda}\mathrm{He} \rightarrow {}^{5}_{\Lambda}\mathrm{He}\pi$

Backups

Model parameters

- Coalescence takes place if the spacial coordinates and relative momenta of constituents are within a spere of radius (Δr, Δp)
  - JAM + coalescence:

	Δr **[fm]**	Δp **[GeV/c]**
d	4.5	0.3
t	4	0.3
H3L	4	0.12
H4L	4	0.3

  - UrQMD cascade + coalescence in slide 14:

	Δr **[fm]**	Δp **[GeV/c]**
d	3.7	0.3
t/He3	3.3	0.3
He4	3.4	0.3
H3L	4	0.15
H4L	4	0.25

  - UrQMD+ coalescence in slide 16：

	Δr **[fm]**	Δp **[GeV/c]**
NN	3.575	0.285
NNΛ	9.5	0.135
NNΛ	4.3	0.25